

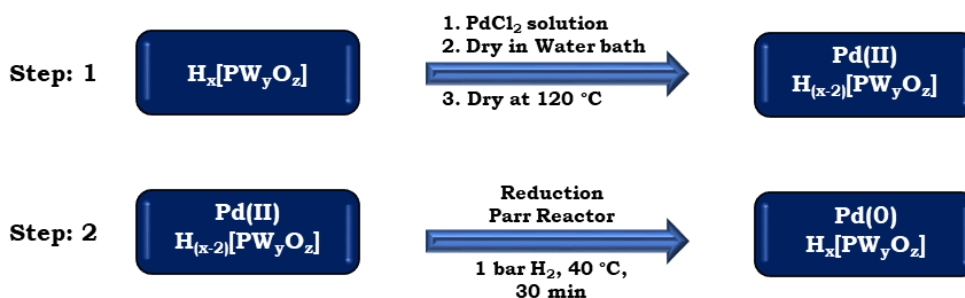
PART-B

Salt Method

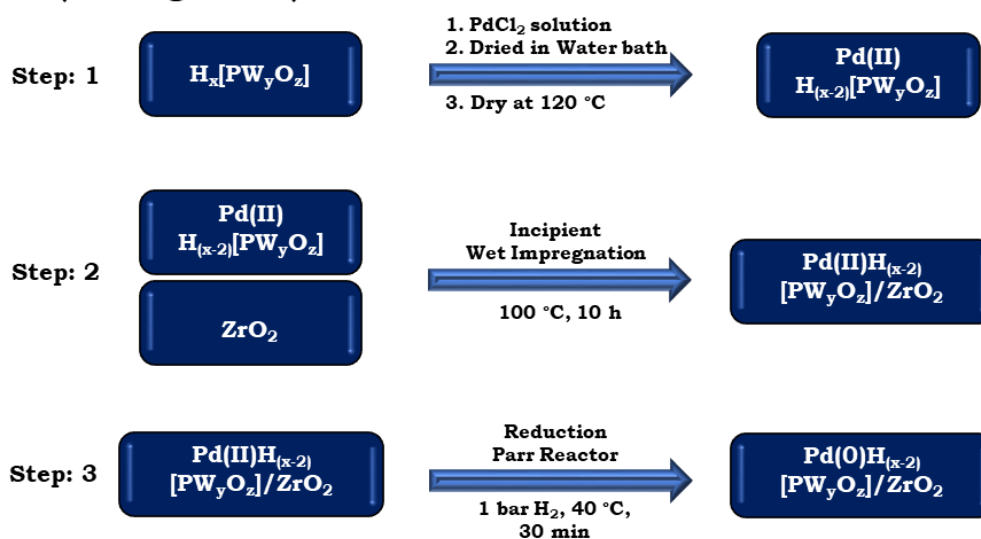
Designing of catalyst by salt method

This method involves two steps for the synthesis of TPA/LTPA stabilized PdNCLs as homogeneous. *Step-I*: The saturated solutions of TPA/LTPA and PdCl_2 are mixed in stoichiometric amount to form Pd(II) salt of TPA/LTPA by evaporation, followed by drying. *Step-II*: Finally, this salt is converted to stabilized PdNCLs by reducing in Parr reactor. This homogeneous counter-part, Pd(II)TPA/LTPA salt can be heterogenized by supporting it over zirconia by incipient wet impregnation method as discussed in general introduction. Synthetic scheme by salt method is given in scheme 1, where, $\text{H}_x[\text{PW}_y\text{O}_z] = 12$ -tungstophosphoric acid, TPA ($\text{H}_3\text{PW}_{12}\text{O}_{40}$) or Mono lacunary tungstophosphoric acid, LTPA ($\text{H}_7\text{PW}_{11}\text{O}_{39}$).

[1] Stabilized PdNCLs by Heteropoly acids (Homogeneous)



[2] Zirconia Supported Stabilized PdNCLs by Heteropoly acids (Heterogeneous)



Scheme 1 Synthetic scheme for stabilized PdNCLs via salt method.

CHAPTER 1

Stabilized PdNCLs by TPA:
Synthesis, Characterization
and Applications to C-C
coupling and Hydrogenation

Metal salt of heteropoly acids (HPAs) have gained tremendous attention as catalysts over the last four decades because they blend the advantages of both, metal as well as HPAs. As discussed in general introduction, HPAs are discrete early transition metal-oxide cluster anions [1] having unrivaled versatility, structural variation in both symmetry and size as well as applications in many fields of science [2]. A wide range of different metal salts of various HPAs can be obtained by exchanging the available counter protons present in their primary structure. In this context, number of articles have been reported using different metals such as Ag [3], Al [4], Cs [5], Cu [6], Fe [7], Ga [8], Hf [9], Sm [10], Sn [11], Ti [12], Zn [13] and Zr [14].

Even though, historically, Pd has been dominant over other metals as a central tool for innumerable organic transformations [15], only three reports are available on Pd salt of HPAs in art. In 1984, Ono et al. reported Pd salt of 12-tungstophosphate ($\text{Pd}_3(\text{PW}_{12}\text{O}_{40})_2$) and its heterogenization over silica-gel for the isomerization of pentane and hexane in the presence of hydrogen [16]. Second in 1989, Maksimov and his co-workers reported exchange of only one proton of 12-tungstophosphoric acid to synthesize $\text{Pd}_{0.5}\text{H}_2\text{PW}_{12}\text{O}_{40}$ and evaluated its catalytic activity in the liquid phase synthesis of methyl tert-butyl ether [17]. Finally in 1995, Stobbe-Kreemers et al. reported Pd salts of parent as well as vanadium substituted molybdophosphoric acid series ($\text{H}_{3+n}\text{PV}_n\text{Mo}_{12-n}\text{O}_{40}$) for the application of gas phase Wacker oxidation of 1-butene [18]. Thus, a literature survey shows that since last 25 years, no further study has been carried out on Pd salt of 12-tungstophosphoric acid. So, it was thought to use the same as a source for generating *in situ* PdNCLs.

In this chapter, **we discuss**, *in situ* synthesis of stabilized PdNCLs consisting TPA (PdTPA) from Pd salt of 12-tungstophosphoric acid (PdHTPA). The synthesized catalyst was characterized by various physico-chemical techniques such as elemental analysis (EDX), TGA, FT-IR, ^{31}P MAS NMR, XRD, XPS and TEM. The

catalytic efficiency was evaluated for C-C coupling (SM and Heck) and hydrogenation reactions. *The catalyst was found to be homogeneous.*

EXPERIMENTAL

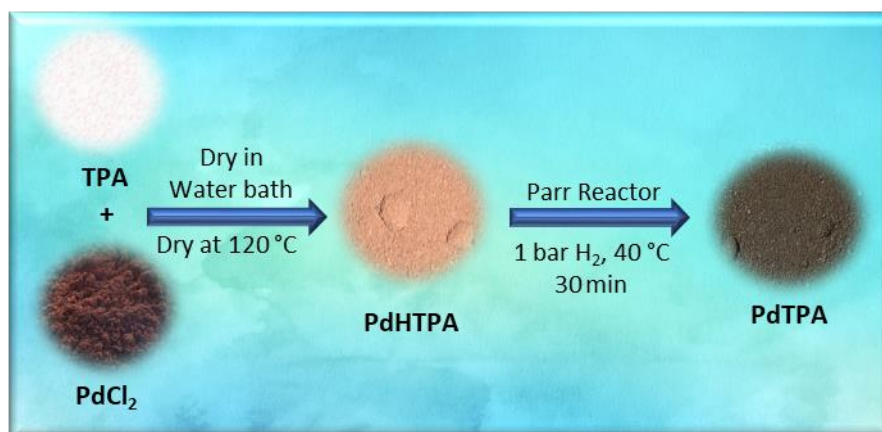
Materials

All chemicals used were of A. R. grade. 12-tungstophosphoric acid, palladium chloride, iodobenzene, phenylboronic acid, styrene, dimethyl formamide, potassium carbonate, cyclohexene, petroleum ether, ethyl acetate and dichloromethane were obtained from Merck and used as received.

Catalyst Synthesis

Stabilized palladium nanoclusters by 12-tungstophosphoric acid (PdTPA) was synthesized by top-down approach (Scheme 1).

Palladium tungstophosphate was synthesized by reported method in literature [10] with modifications. 1 g of TPA was dissolved in minimum amount of distilled water followed by the addition of a stoichiometric amount of aqueous PdCl₂ (58.6 mg) solution dropwise. The resulting mixture was aged for 1 h at 80 °C and the excess water was evaporated to dryness on the water bath. The resulting material was oven dried at 120 °C overnight to obtain brown coloured salt, designated as PdHTPA. In this step, available protons of TPA get replaced by Pd(II) in stoichiometric amount. Finally, PdHTPA was reduced under 1 bar H₂ pressure at 40 °C for 30 min in Parr reactor and the obtained black coloured catalyst was designated as PdTPA.



Scheme 1 Synthesis of PdTPA.

Catalytic Evaluation

The C-C Coupling and hydrogenation reactions were carried out following the same procedure as mentioned in Part-A_Chapter 1.

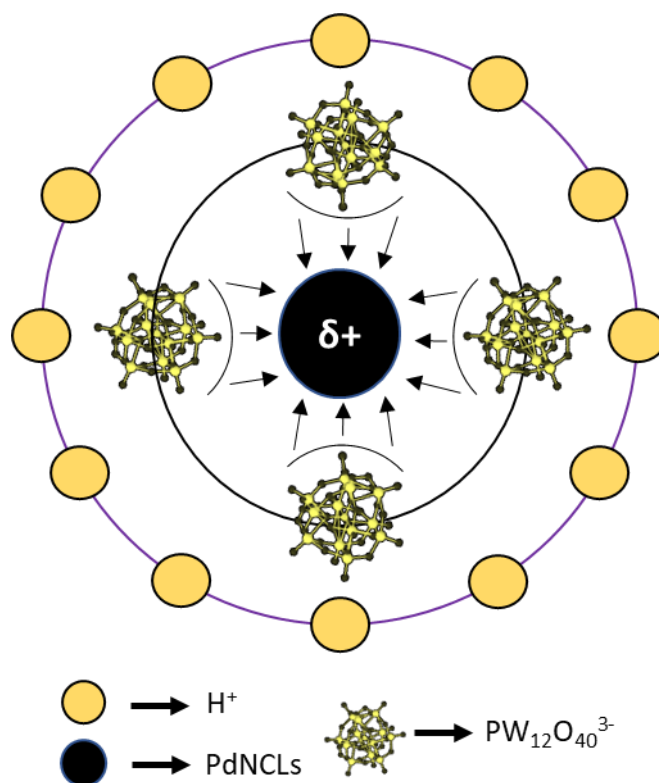
RESULTS AND DISCUSSION

Stabilization Mechanism of PdNCLs by TPA

It is well known that generally stabilization of metal nanoclusters (MNCLs) involves mainly two models [19]: (i) Electrostatic (Coulombic) repulsion to stabilize MNCLs by opposing van der Waals attraction between the particles, responsible for agglomeration [20-22], and (ii) steric repulsion [23-25] by added polymers, bulky cations/anions.

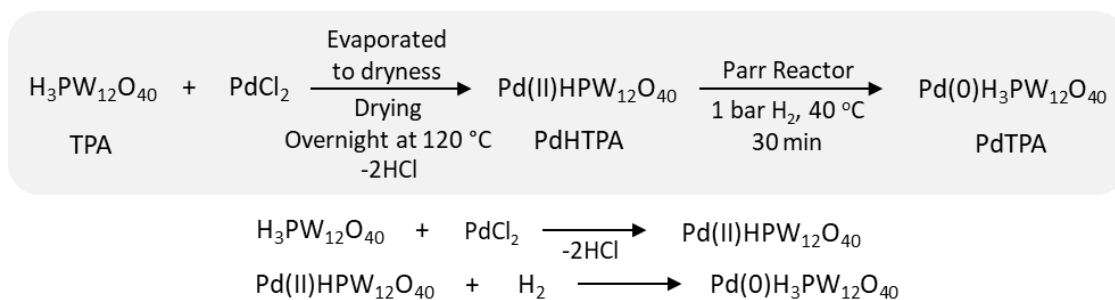
It is also reported in literature that negative charge associated with the heteropoly anion and a second layer of positive charges (in the present case, hydrogen) are capable of stabilizing the metal clusters following the first model. Keggin derivatives bind to the metal surface through terminal oxygen's (which possess C₃ symmetry, tridentate, facial array of oxygen atoms for coordination to the metal(0) surface) [19]. Here also, we can presume that the negative charge associated with the oxygen (terminal) of heteropoly anion electrostatically attracts the PdNCLs by layer formation to prevent it from agglomeration into

bulk. And finally, this negative charge gets neutralized electrically by the counter protons of HPAs by formation of second layer [26] as shown in scheme 2.



Scheme 2 Stabilization of PdNCLs by TPA in PdTPA.

The stabilized metal-clusters have been synthesized *in-situ* via reduction in presence of H_2 and a possible mechanism is proposed Scheme 3. However, it is difficult to comment anything about the preferred binding sites. *Here, we assume that some terminal oxygens are still available for bonding.*



Scheme 3 Mechanism of PdNCLs stabilization.

Catalyst Characterization

The gravimetric analysis of Pd (3.52 wt %) and W (74.40 wt %) for PdTPA are in good agreement with the theoretical values (3.60 wt % and 74.59 wt %, respectively) as well as EDX values (3.46 wt % and 74.87 wt %, respectively). EDX elemental mapping of the catalyst is shown in figure 1.

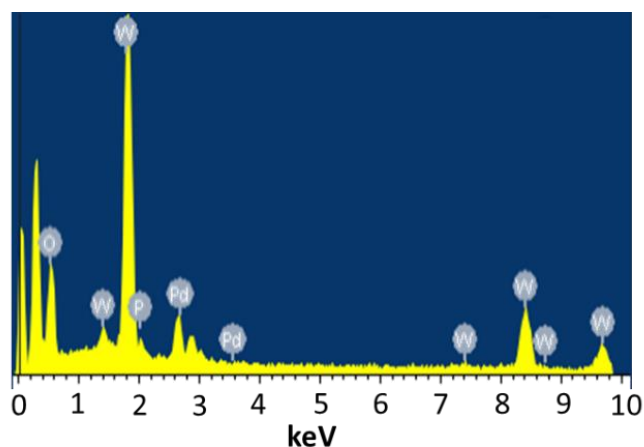


Figure 1 EDX mapping.

TGA of PdTPA (Figure 2) shows 0.8 % weight loss attributed to adsorbed water, in the temperature range of 70-120 °C, while 3.0 % weight loss up to 190 °C, indicating the loss of crystalline water molecules. Further, no weight loss was observed indicating that synthesized catalyst is thermally stable up to 350 °C.

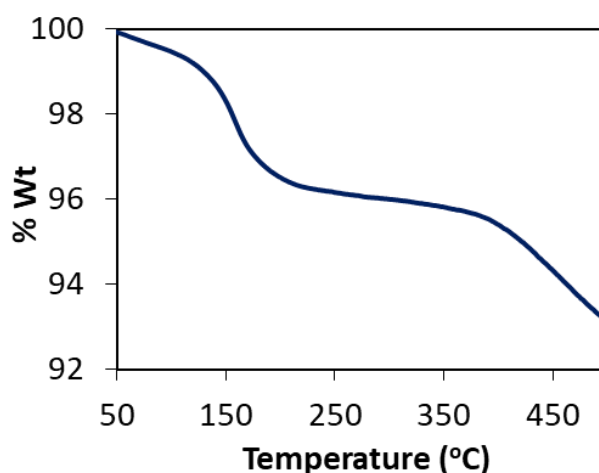


Figure 2 TGA curve.

The FT-IR spectra of TPA and PdTPA are shown in figure 3. TPA shows its characteristic bands at 1088, 987, 893 and 800 cm^{-1} corresponding to P-O, W=O and W-O-W stretching, respectively (Figure 3a). PdTPA (Figure 3b) shows bands at 1080, 982, 890 and 795 cm^{-1} corresponding to P-O, W=O, and W-O-W stretching, respectively. Here, the absence of $\nu(\text{P-O})$ splitting into 1088 and 1042 cm^{-1} confirms that Pd has not been incorporated within the Keggin unit [27].

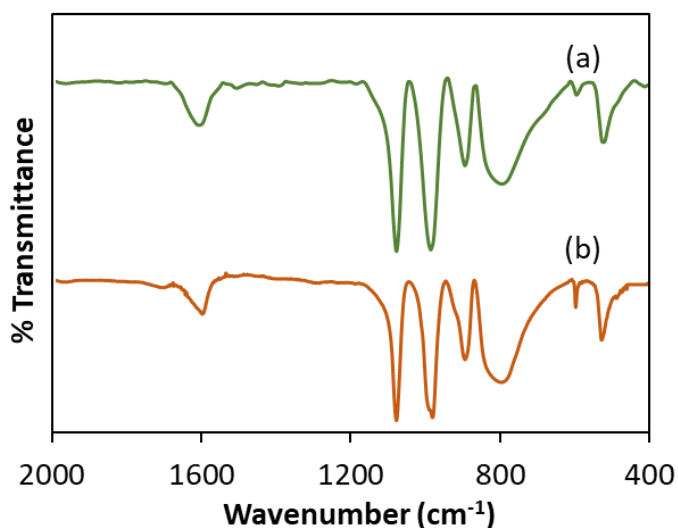


Figure 3 FT-IR spectra of (a) TPA and (b) PdTPA.

^{31}P MAS NMR spectra of TPA and PdTPA are presented in figure 4 to understand the chemical environment around phosphorus [28]. Pure TPA

shows a single peak at -15.62 ppm, which is in good agreement with the reported one [29]. PdTPA shows an intense peak at -14.31 ppm, and the observed low shift indicates that there is no significant effect of Pd on the electronic environment of phosphorus in TPA. The obtained value is different from the reported chemical shifts for LTPA (mono lacunary tungstophosphoric acid, -11.3 ppm) [30], confirming the absence of any lacunary structure as well as the presence of Pd as a counter species only.

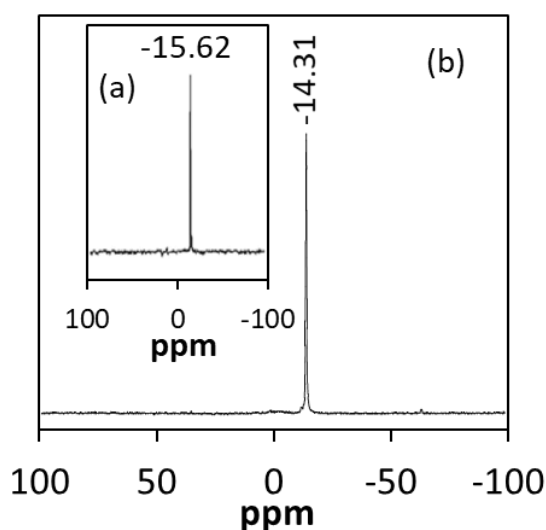


Figure 4 ^{31}P MAS NMR of (a)TPA and (b) PdTPA.

XRD patterns of TPA and PdTPA were recorded as shown in figure 5. XRD of PdTPA shows all the characteristic peaks within the range 15-25 degree 2θ corresponding to TPA. Moreover, four additional reflections were observed at 38.5, 47.3, 59.8 and 68.1 degrees 2θ that could be attributed to 111, 200, 220 and 311 planes of elemental palladium.

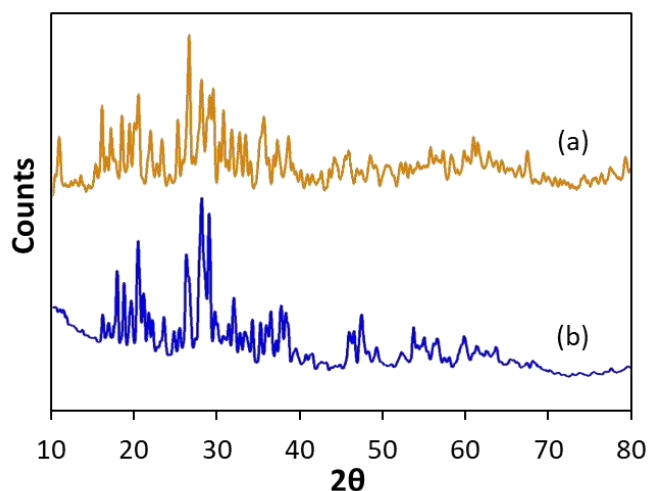


Figure 5 Powder XRD patterns of (a) TPA and (b) PdTPA.

To confirm the oxidation states of Pd and W, the XPS spectrum of PdTPA was recorded (Figure 6). The reported binding energy values of Pd(0) are 532.4 eV, 335.2 eV and 340.5 eV corresponding to Pd3p_{3/2}, Pd3d_{5/2} and Pd3d_{3/2} respectively [31, 32], whereas for Keggin type HPAs, binding energy values for W(VI) are 35.6 eV and 37.8 eV corresponding to W4f_{7/2} and W4f_{5/2} respectively [33]. The XPS spectrum of PdTPA shows a very intense peak at 532 eV (Pd3p_{3/2} and O1s), which is in good agreement with the well-known fact that there is direct overlap between Pd3p_{3/2} and O1s peaks [34], and cannot be assigned to confirm the presence of Pd(0). Hence, we have presented instrument generated full spectrum image supporting the presence of Pd(0). This was further confirmed by recording the high resolution Pd3d and W4f XPS spectra of the catalyst. It shows a spin orbit doublet peak of Pd3d at binding energy 335.9 eV (3d_{5/2}) and 340.9 eV (3d_{3/2}), confirming the presence of Pd(0) [26, 35-37]. The W4f peak is composed of a well resolved spin orbit doublet at 34.5 eV and 36.7 eV correspond to W4f_{7/2} and W4f_{5/2} respectively, typical of W(VI), in agreement with literature data on Keggin-type HPAs [36, 38], confirming that W(VI) is not reduced.

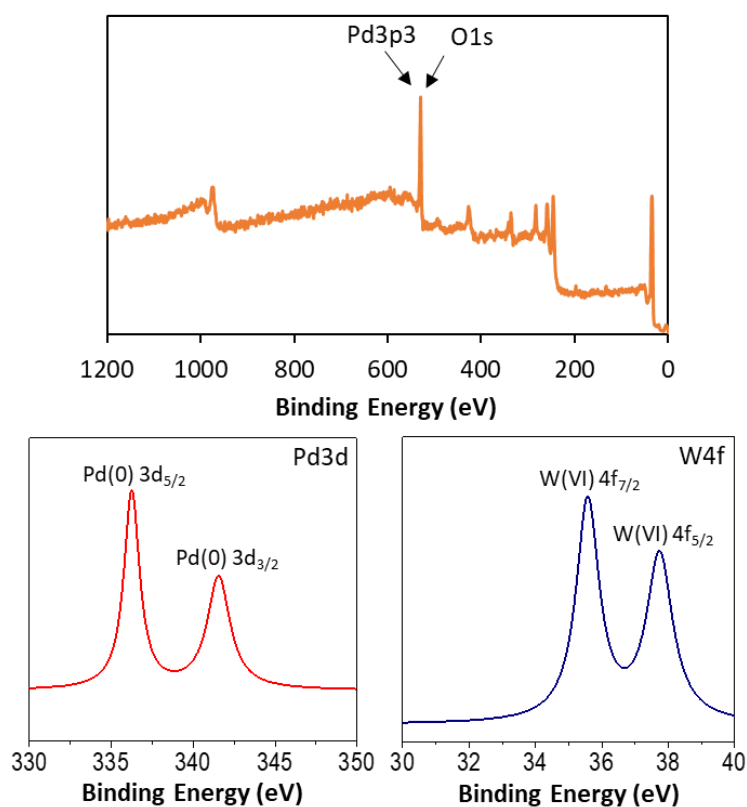


Figure 6 XPS spectra of PdTPA.

TEM image of PdTPA is presented in figure 7. Image clearly shows the presence of highly dispersed Pd(0) NCLs (~2 nm). Moreover, no any aggregates formation of Pd as well as TPA crystallization is observed, which confirms the stabilization of PdNCLs by TPA.

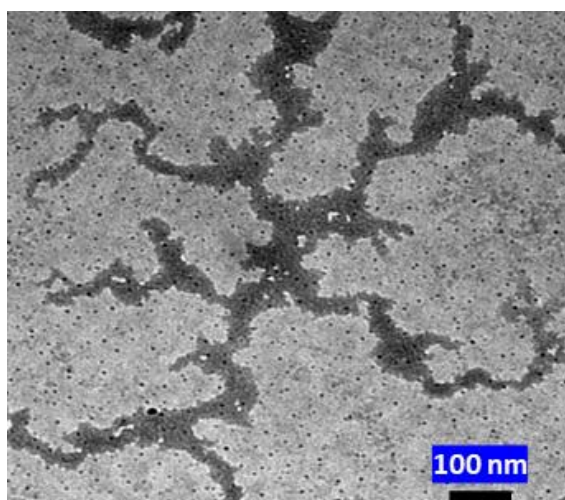


Figure 7 TEM images of PdTPA.

FT-IR and ^{31}P MAS NMR data show that TPA structure remains intact even after post reduction of the catalyst. XPS confirms the presence of Pd and W in 0 and VI oxidation states, respectively, whereas TEM exposes the homogeneous dispersion of PdNCLs.

C-C Coupling and Hydrogenation

The preliminary study of catalyst efficiency towards C-C coupling (SM and Heck) as well as hydrogenation reactions were carried out and obtained results are shown in table 1. The catalyst is homogeneous and highly active towards the said reactions. However, after reactions, formation of black particles (Pd black) was observed as shown in figure with table 1, suggesting that PdNCLs may have leached out from the catalyst. To confirm the same, recycle study was carried out before proceeding towards optimization.

Table 1 Activity of the catalyst

Reaction	% Conversion
^a SM	96
^b Heck	96
^c Hydrogenation	91



Reaction conditions: (a) *SM coupling*- iodobenzene (1.96 mmol), phenylboronic acid (2.94 mmol), K_2CO_3 (3.92 mmol), conc. of Pd (3.76×10^{-4} mmol, 0.0192 mol%), $\text{C}_2\text{H}_5\text{OH}:\text{H}_2\text{O}$ (3:7 mL), time (30 min), temperature (90 °C), (b) *Heck coupling*- iodobenzene (0.98 mmol), styrene (1.47 mmol), K_2CO_3 (1.96 mmol), conc. of Pd (1.13×10^{-3} mmol, 0.115 mol%), $\text{DMF}:\text{H}_2\text{O}$ (3:2 mL), time (6 h), temperature (100 °C), (c) *Hydrogenation*- cyclohexene (9.87 mmol), conc. of Pd (1.50×10^{-3} mmol, 0.015 mol%), H_2O (50 mL), time (4 h), temperature (80 °C), H_2 pressure (10 bar): (d) Leaching of PdNCLs from the catalyst during the reaction.

Recycling and sustainability of the catalyst

The recovery and recycling of the catalyst is a key issue for the sustainability of any catalytic process. Considering this, the catalyst was first screened for

recycling test. For the same, after reaction completion, the organic layer was extracted by dichloromethane and aqueous layer was recovered for the use of next catalytic run directly. Obtained results (Figure 8) show the drastic deactivation of catalyst in consequent runs for all the reactions, confirming the leaching of PdNCLs from the catalyst.

The negative results obtained in the form of leaching made us reconsider the synthetic procedure and redesign the catalyst to overcome the sustainability issue.

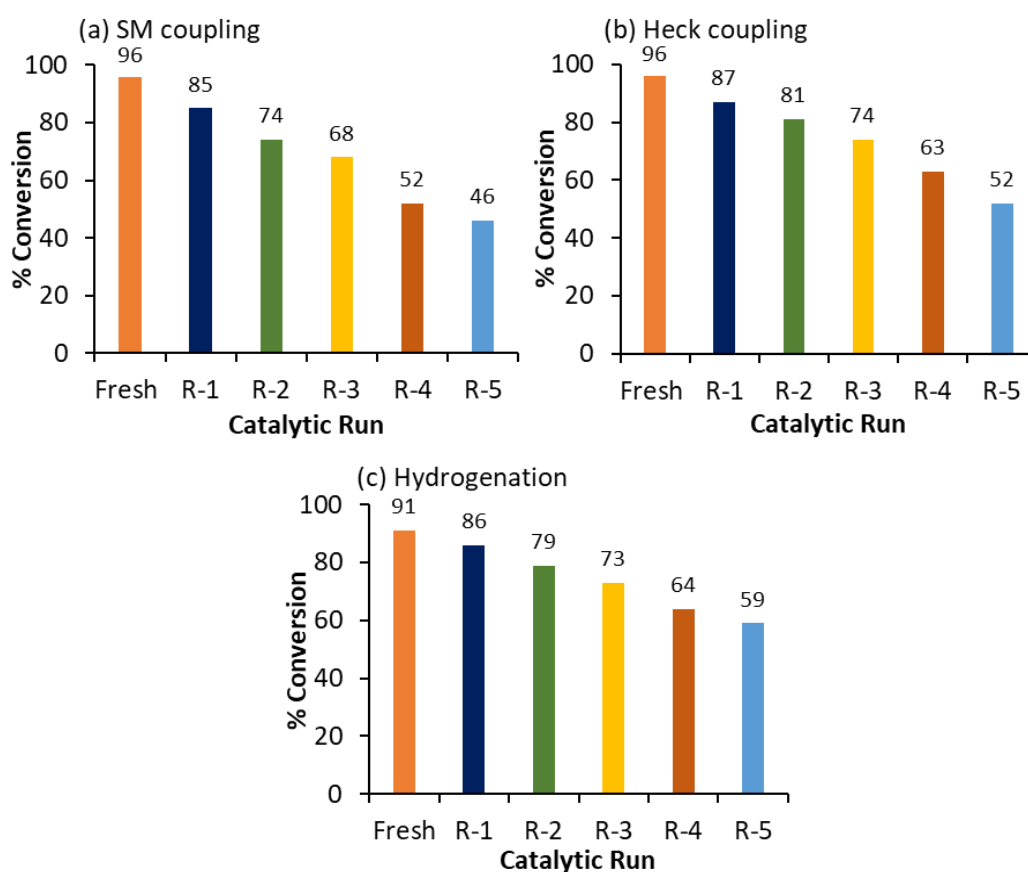


Figure 8 Reaction conditions: (a) *SM coupling*- iodobenzene (1.96 mmol), phenylboronic acid (2.94 mmol), K_2CO_3 (3.92 mmol), conc. of Pd (3.76×10^{-4} mmol, 0.0192 mol%), $C_2H_5OH:H_2O$ (3:7 mL), time (30 min), temperature (90 °C); (b) *Heck coupling*- iodobenzene (0.98 mmol), styrene (1.47 mmol), K_2CO_3 (1.96 mmol), conc. of Pd (1.13×10^{-3} mmol, 0.115 mol%), $DMF:H_2O$ (3:2 mL), time (6 h), temperature (100 °C); (c) *Hydrogenation*- cyclohexene (9.87 mmol), conc. of Pd (1.50×10^{-3} mmol, 0.015 mol%), H_2O (50 mL), time (4 h), temperature (80 °C), H_2 pressure (10 bar).

Conclusion

- Synthesis of stabilized PdNCLs by 12-tungstophosphoric acid (PdTPA) was carried successfully
- Synthesized material was characterized by elemental analysis (EDX), TGA, FT-IR, ^{31}P MAS NMR, XRD, XPS and TEM
 - FT-IR, XRD and ^{31}P MAS NMR show the retention of Keggin structure
 - XPS confirms the oxidation state of Pd(0) and W(VI)
 - TEM reveals the homogeneous dispersion of PdNCLs
- The catalyst gives excellent % conversion for C-C coupling (SM and Heck) and hydrogenation reactions in homogeneous medium
- Recycling confirms the **leaching of PdNCLs** from the catalyst and hence designing of heterogeneous catalyst is necessary

Note: This work has been published in **Catalysis Letters** (Designing of Highly Active and Sustainable Encapsulated Stabilized Palladium Nanoclusters as well as Real Exploitation for Catalytic Hydrogenation in Water, Anish Patel and Anjali Patel, Catal. Lett., 2020, DOI: 10.1007/s10562-020-03327-4). The front page of accepted manuscript is presented in the annexure section.

References

- [1] K. Fukaya and T. Yamase, *Angew. Chem.*, 115, 678-682, (2003).
- [2] N. Narkhede, S. Singh and A. Patel, *Green. Chem.*, 17, 89-107, (2015).
- [3] J. S. Yadav, B. V. S. Reddy, S. Praveenkumar, K. Nagaiah, N. Lingaiah and P. S. Saiprasad, *Synthesis*, 2004, 901-904, (2004).
- [4] K. Mohan Reddy, N. Seshu Babu, P. S. Sai Prasad and N. Lingaiah, *Catal. Commun.*, 9, 2525-2531, (2008).
- [5] K. Srilatha, R. Sree, B. L. A. Prabhavathi Devi, P. S. Sai Prasad, R. B. N. Prasad and N. Lingaiah, *Bioresour. Technol.*, 116, 53-57, (2012).
- [6] N. Pasha, N. Seshu Babu, K. T. Venkateswara Rao, P. S. Sai Prasad and N. Lingaiah, *Tetrahedron Lett.*, 50, 239-242, (2009).
- [7] K. T. Venkateswara Rao, P. S. Sai Prasad and N. Lingaiah, *J. Mol. Catal. A: Chem.*, 312, 65-69, (2009).
- [8] C. Ramesh Kumar, S. M and N. Lingaiah, *Appl. Catal., A*, 487, 165-171, (2014).
- [9] C. R. Kumar, N. Rambabu, N. Lingaiah, P. S. S. Prasad and A. K. Dalai, *Appl. Catal., A*, 471, 1-11, (2014).
- [10] C. R. Kumar, K. Jagadeeswaraiah, P. S. S. Prasad and N. Lingaiah, *ChemCatChem*, 4, 1360-1367, (2012).
- [11] C. Ramesh Kumar, K. T. V. Rao, P. S. Sai Prasad and N. Lingaiah, *J. Mol. Catal. A: Chem.*, 337, 17-24, (2011).
- [12] B. S. Rao, P. K. Kumari, D. D. Lakshmi and N. Lingaiah, *Catal. Today*, 309, 269-275, (2018).
- [13] K. Jagadeeswaraiah, C. R. Kumar, P. S. S. Prasad and N. Lingaiah, *Catal. Sci. Technol.*, 4, 2969-2977, (2014).
- [14] N. Pasha, N. Lingaiah and R. Shiva, *Catal. Lett.*, 149, 2500-2507, (2019).
- [15] Z. Chen, E. Vorobyeva, S. Mitchell, E. Fako, M. A. Ortuño, N. López, S. M. Collins, P. A. Midgley, S. Richard, G. Vilé and J. Pérez-Ramírez, *Net. Nanotechnol.*, 13, 702-707, (2018).
- [16] S. Suzuki, K. Kogai and Y. Ono, *Chem. Lett.*, 13, 699-702, (1984).

-
- [17] G. M. Maksimov and I. V. Kozhevnikov, *React. Kinet. Catal. Lett.*, 39, 317-322, (1989).
- [18] A. W. Stobbekreemers, G. Vanderlans, M. Makkee and J. J. F. Scholten, *J. Catal.*, 154, 187-193, (1995).
- [19] R. G. Finke and S. Özkar, *Coord. Chem. Rev.*, 248, 135-146, (2004).
- [20] D. F. Evans and H. Wennerström, *The Colloidal Domain: Where Physics, Chemistry, Biology, and Technology Meet*, Wiley, (1999).
- [21] C. S. Hirtzel and R. Rajagopalan, *Colloidal phenomena: advanced topics*, Noyes Data Corporation, (1985).
- [22] R. J. Hunter and L. R. White, *Foundations of Colloid Science*, Clarendon Press, (1987).
- [23] J. D. Aiken and R. G. Finke, *J. Mol. Catal. A: Chem.*, 145, 1-44, (1999).
- [24] J. D. Aiken, Y. Lin and R. G. Finke, *J. Mol. Catal. A: Chem.*, 114, 29-51, (1996).
- [25] D. L. Fedlheim and C. A. Foss, *Metal Nanoparticles: Synthesis, Characterization, and Applications*, Taylor & Francis, (2001).
- [26] L. D'Souza, M. Noeske, R. M. Richards and U. Kortz, *Appl. Catal., A*, 453, 262-271, (2013).
- [27] N. Mizuno, J.-S. Min and A. Taguchi, *Chem. Mater.*, 16, 2819-2825, (2004).
- [28] I. Kozhevnikov, K. Kloetstra, A. Sinnema, H. Zandbergen and H. V. Van Bekkum, *J. Mol. Catal. A: Chem.*, 114, 287-298, (1996).
- [29] T. Okuhara, N. Mizuno and M. Misono, *Appl. Catal., A*, 222, 63-77, (2001).
- [30] A. Patel and S. Singh, *Microporous Mesoporous Mater.*, 195, 240-249, (2014).
- [31] T. Fleisch, W. N. Delgass and N. Winograd, *Surf. Interface Anal.*, 3, 23-28, (1981).
- [32] M. C. Militello and S. J. Simko, *Surf. Sci. Spectra*, 3, 387-394, (1994).
- [33] D. Mercier, S. Boujday, C. Annabi, R. Villanneau, C.-M. Pradier and A. Proust, *J. Phys. Chem. C.*, 116, 13217-13224, (2012).
-

- [34] A. V. Matveev, V. V. Kaichev, A. A. Saraev, V. V. Gorodetskii, A. Knop-Gericke, V. I. Bukhtiyarov and B. E. Nieuwenhuys, *Catal. Today*, 244, 29-35, (2015).
- [35] Y. Leng, C. Zhang, B. Liu, M. Liu, P. Jiang and S. Dai, *ChemSusChem*, 11, 3396-3401, (2018).
- [36] R. Villanneau, A. Roucoux, P. Beaunier, D. Brouri and A. Proust, *RSC Adv.*, 4, 26491-26498, (2014).
- [37] L. D'Souza, M. Noeske, R. M. Richards and U. Kortz, *J. Colloid Interface Sci.*, 394, 157-165, (2013).
- [38] S. Rana and K. M. Parida, *Catal. Sci. Technol.*, 2, 979-986, (2012).

CHAPTER 2

Zirconia Supported Stabilized
PdNCLs by TPA: Synthesis,
Characterization and
Applications to C-C coupling
and Hydrogenation

To overcome the leaching of PdNCLs from the homogeneous catalyst PdTPA (please refer, conclusion of Part-B_Chapter-1), and keeping in mind the advantages of supported heterogeneous catalysts, it was thought to make PdTPA heterogeneous by supporting it over the suitable support. In this work, considering the advantages of Zirconia (ZrO_2), as discussed in general introduction, PdTPA was supported onto ZrO_2 by incipient-wet impregnation method.

In this chapter, first time, we report the supporting of PdTPA onto ZrO_2 (PdTPA/ ZrO_2) by impregnation and post reduction method. The synthesized catalyst was characterized by EDX, TGA, BET, FT-IR, ^{31}P MAS NMR, powder XRD, XPS, TEM, HRTEM and BF/DF-STEM. The efficiency of the catalyst was evaluated as a sustainable heterogeneous catalyst for C-C coupling (SM and Heck) and hydrogenation. Influence of various parameters such as catalyst amount, temperature, pressure, time, base, solvent, solvent ratio was studied for each reaction to obtain maximum conversion. The catalyst was retrieved by simple centrifugation, regenerated at 100 °C by drying and reused up to five cycles. The regenerated catalyst was characterized by EDS, FT-IR, XRD, BET and XPS to confirm its sustainability. The viability was examined towards different substrates as well as comparison with previously reported systems was also surveyed.

EXPERIMENTAL

Materials

All chemicals used were of A. R. grade. 12-tungstophosphoric acid, zirconium oxychloride, 25 % (w/v) ammonia, palladium chloride, iodobenzene, phenylboronic acid, styrene, dimethyl formamide, potassium carbonate, cyclohexene, petroleum ether, ethyl acetate and dichloromethane were obtained from Merck and used as received.

Catalyst Synthesis

Zirconia supported stabilized palladium nanoclusters by 12-tungstophosphoric acid (PdTPA/ZrO₂) was synthesized by top-down approach in three steps.

Step-1: Synthesis of Zirconia (ZrO₂)

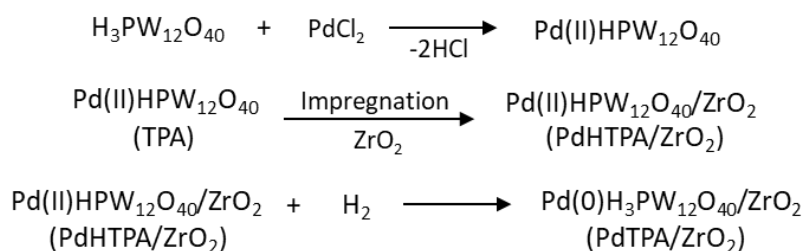
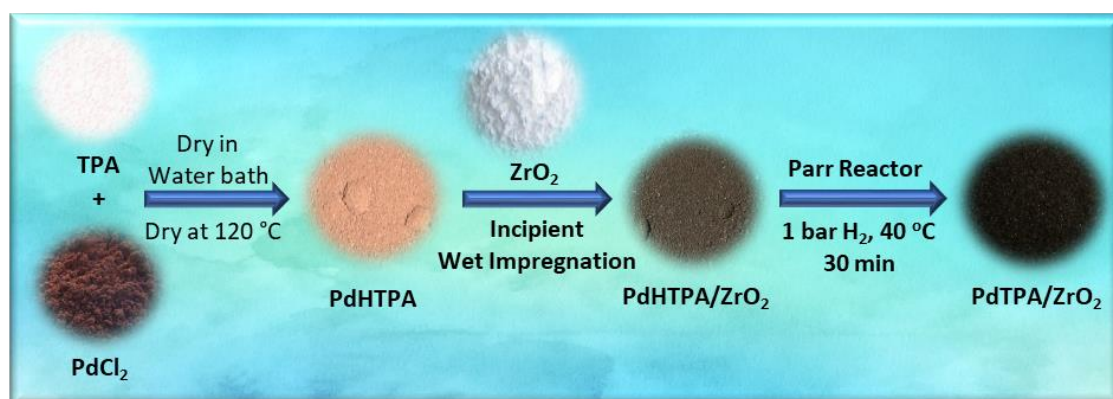
ZrO₂ was synthesized as discussed in Part-A_Chapter-1.

Step-2: Synthesis of Palladium tungstophosphate (PdHTPA).

PdHTPA was synthesized as discussed in Part-B_Chapter-1.

Step-3: Synthesis of PdTPA supported onto Zirconia (PdTPA/ZrO₂).

A series of catalysts, containing 10-40 % of PdHTPA supported onto ZrO₂ was synthesized by incipient wet impregnation method. 1 g of ZrO₂ was impregnated with aqueous solution of PdHTPA (0.1/10-0.4/40 g mL⁻¹ of double distilled water) and dried at 100 °C for 10 h and finally treated under 1 bar H₂ pressure at 40 °C for 30 min using Parr reactor. The obtained catalysts with 10-40 % loading were coded as 10 % PdTPA/ZrO₂, 20 % PdTPA/ZrO₂, 30 % PdTPA/ZrO₂ (Later, PdTPA/ZrO₂) and 40 % PdTPA/ZrO₂, respectively. The synthetic scheme of PdTPA/ZrO₂ is shown in scheme 1.



Scheme 1 Synthesis of PdTPA/ZrO₂.

Catalytic Evaluation

The C-C Coupling and hydrogenation reactions were carried out following the same procedure as mentioned in Part-A_Chapter 1.

The effect of loading on said reactions was evaluated for all four catalysts. The obtained results (Figure 1) show that conversion increases with increase in % loading from 10 % to 30 % PdTPA and slightly decreases for 40 % loading indicating the blocking of active sites in catalyst. Hence, 30% PdTPA/ZrO₂ catalyst was selected for detailed characterization and catalytic study, and recoded as PdTPA/ZrO₂.

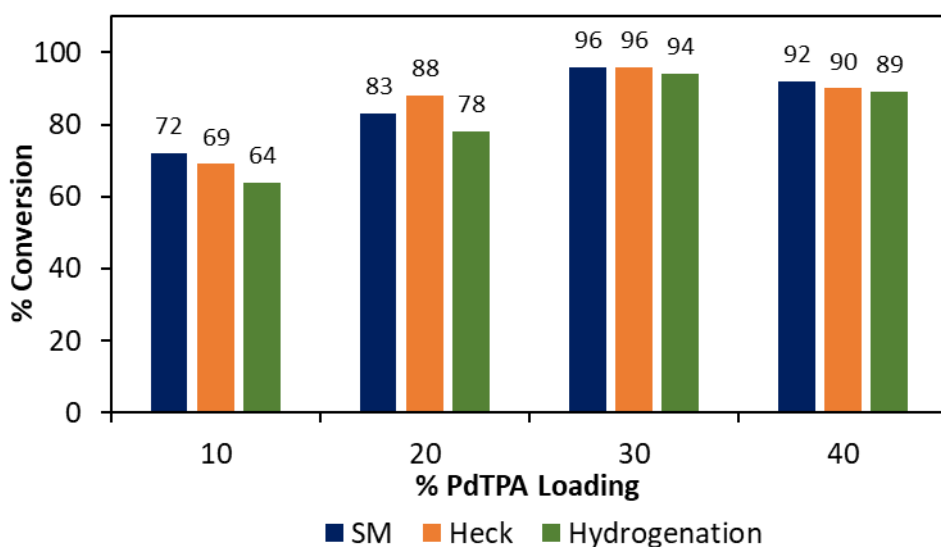


Figure 1 Effect of % PdTPA loading. Reaction condition: *SM coupling*- iodobenzene (1.96 mM), phenylboronic acid (2.94 mM), catalyst (0.0192 mol% Pd), K_2CO_3 (3.92 mmol), C_2H_5OH : H_2O (3:7 mL), temperature (90 °C), time (30 min); *Heck coupling*- iodobenzene (0.98 mM), styrene (1.47 mM), catalyst (0.115 mol% Pd), K_2CO_3 (1.96 mmol), DMF: H_2O (3:2 mL), temperature (100 °C), time (6 h); *Hydrogenation*- cyclohexene (9.87 mmol), catalyst (0.023 mol% Pd), H_2O (50 mL), temperature (50 °C), H_2 pressure (8 bar), time (4 h).

RESULTS AND DISCUSSION

Catalyst Characterization

The gravimetric analysis of Pd (3.52 wt %) and W (74.40 wt %) for PdTPA are in good agreement with the theoretical values (3.60 wt % and 74.59 wt %, respectively) as well as EDX values (3.46 wt % and 74.87 wt %, respectively). For PdTPA/ZrO₂, EDX values for W (17.36 wt %) and Pd (0.80 wt %) are also in good agreement with theoretical values, W (17.21 wt %) and Pd (0.82 wt %). EDX elemental mapping of the catalysts is shown in figure 2.

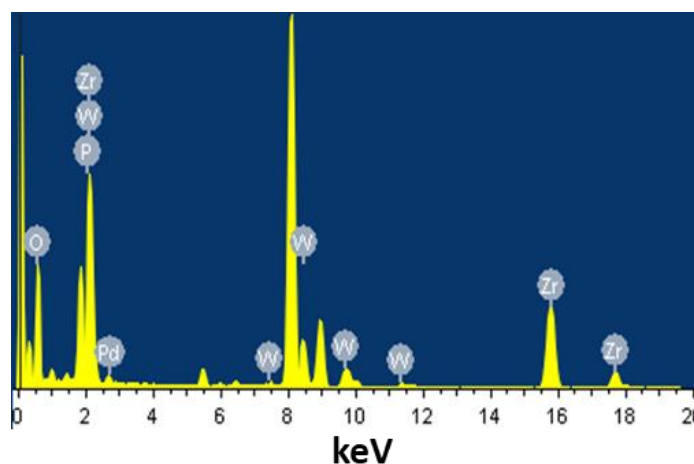


Figure 2 EDX mapping.

TGA of PdTPA (Figure 3) shows 0.8 % weight loss attributed to adsorb water, in the temperature range of 70-120 °C. While, 3.0 % weight loss up to 190 °C, indicating the loss of crystalline water molecules. Whereas, PdTPA/ZrO₂ shows an initial weight loss of 4.3 % up to 120 °C, indicating the loss of adsorbed water molecules. Beside this, no significant weight loss up to 500 °C, indicating higher thermal stability of the catalyst.

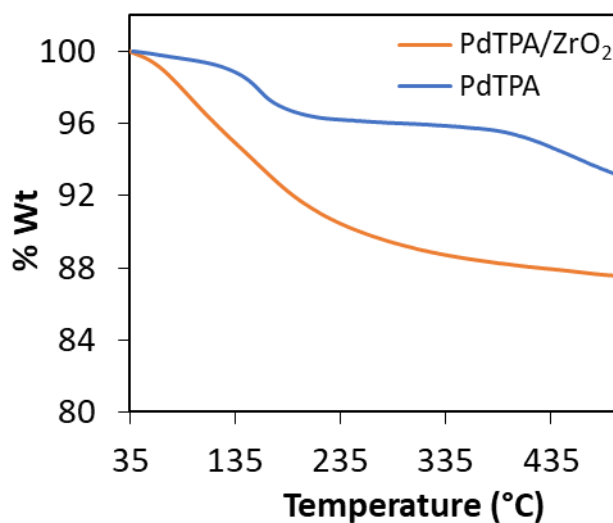


Figure 3 TGA curves.

The FT-IR spectra of TPA, PdTPA, ZrO₂ and PdTPA/ZrO₂ are shown in figure 4. TPA shows its characteristic bands at 1088, 987, 893 and 800 cm⁻¹ corresponding to P-O, W=O and W-O-W stretching, respectively (Figure 4a). Whereas, PdTPA (Figure 4b) shows bands at 1080, 982, 890 and 795 cm⁻¹ corresponding to P-O, W=O, and W-O-W stretching, respectively. Here, absence of $\nu(\text{P-O})$ splitting into 1088 and 1042 cm⁻¹ confirms the presence of Pd as counterpart only [1]. ZrO₂ shows broad bands (Figure 4c) in the region of 1600, 1370, and 600 cm⁻¹ attributed to H-O-H and O-H-O bending and Zr-OH bending, respectively. FT-IR spectrum of PdTPA/ZrO₂ (Figure 4d) exhibits bands at 1078, 978, 888 and 802 cm⁻¹ corresponding to P-O, W=O and W-O-W stretching vibration frequencies, respectively. Here, the disappearance of band at 1370 cm⁻¹ indicates the interaction, between support and PdTPA without alteration in the basic structure of Keggin unit.

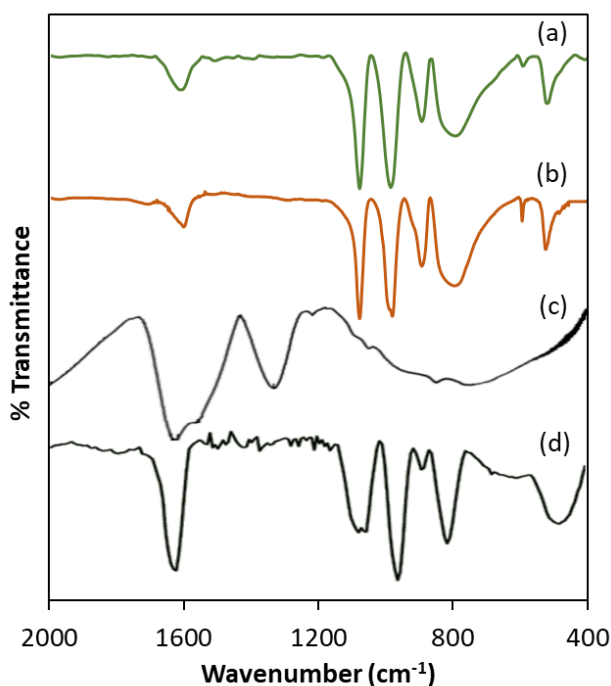


Figure 4 FT-IR spectra of (a) TPA, (b) PdTPA, (c) ZrO₂ and (d) PdTPA/ZrO₂.

³¹P MAS NMR spectra of TPA, PdTPA and PdTPA/ZrO₂ are presented in figure 5 to understand the chemical environment around phosphorus as well as the interaction of anion with support [2]. Pure TPA shows a single peak at -15.62 ppm, which is in good agreement with the reported one [3]. PdTPA shows an intense peak at -14.31 ppm, here, the observed slight shift indicates that there is no significant effect of Pd on the electronic environment of phosphorus in TPA. Whereas, shifting for PdTPA/ZrO₂ at -12.47 ppm may be due the interaction of PdTPA and surface of ZrO₂ [4]. The obtained value is different from the reported chemical shifts for LTPA (mono lacunary tungstophosphoric acid, -11.3 ppm) [5], confirming the absence of any lacunary structure as well as the presence of Pd as a counter species only.

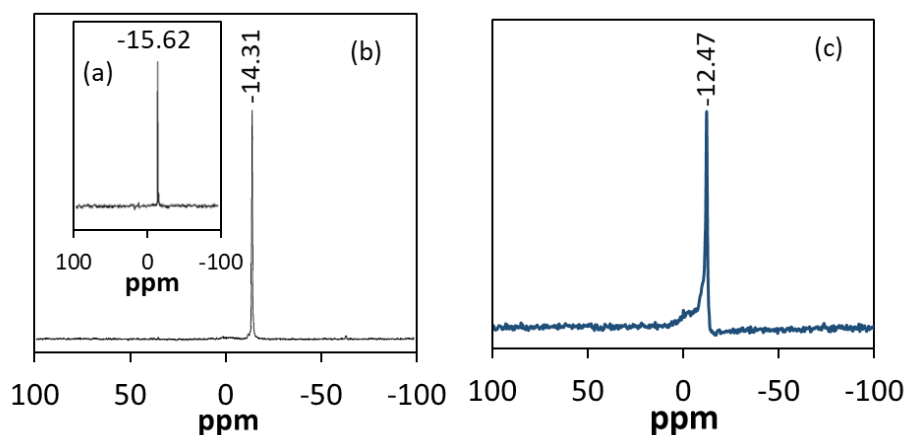


Figure 5 ^{31}P MAS NMR of (a) TPA, (b) PdTPA and (c) PdTPA/ZrO₂.

XRD patterns of TPA, PdTPA, ZrO₂ and PdTPA/ZrO₂ were recorded in order to study the dispersion of active species onto surface of support (Figure 6). XRD of PdTPA shows all the patterns correspond to TPA, indicating the retention of TPA structure. Moreover, four additional reflections are observed at degree 2θ of 38.5, 47.3, 59.8 and 68.1 that could be attributed to 111, 200, 220 and 311 planes of Pd(0). ZrO₂ shows the characteristic broad peak between 20-30, degree 2θ . Whereas, in XRD patterns of PdTPA/ZrO₂, absence of any crystalline peak reveals the homogeneous dispersion of PdTPA onto surface of ZrO₂.

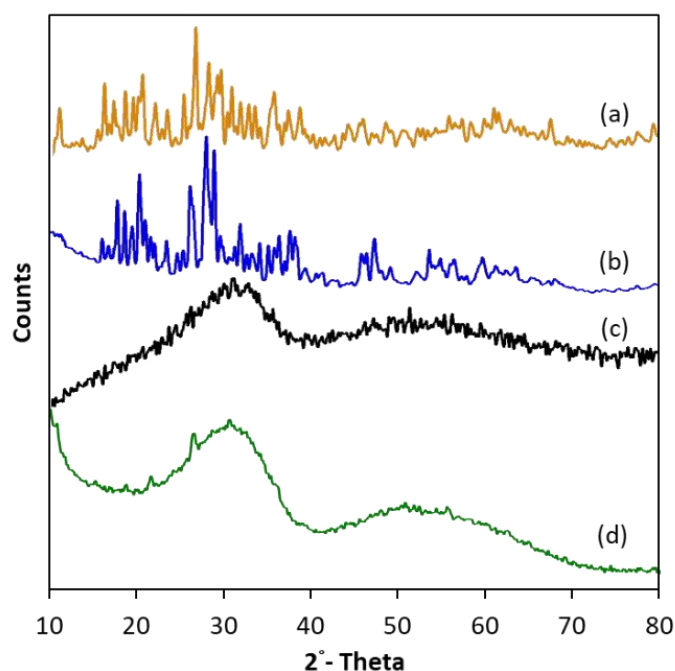


Figure 6 Powder XRD patterns of (a) TPA, (b) PdTPA, (c) ZrO_2 and (d) PdTPA/ ZrO_2 .

The value for BET surface area of ZrO_2 was found to be $170 \text{ m}^2/\text{g}$, while, that of PdTPA/ ZrO_2 was $202 \text{ m}^2/\text{g}$. The observed drastic increase in surface area is due to the presence of PdNCLs onto surface of ZrO_2 . The identical N_2 sorption isotherms (Figure 7) for both, support and designed catalyst, indicating the retention of basic nature of the catalyst even after impregnation and post reduction treatment.

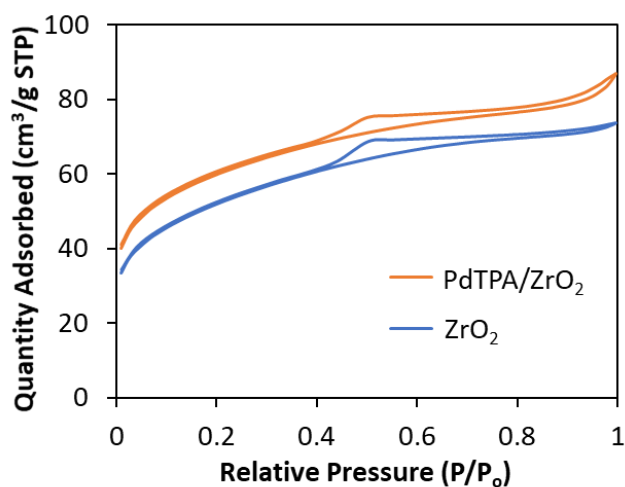


Figure 7 N_2 sorption isotherms.

To confirm the oxidation states of Pd and W, the XPS spectra of PdTPA and PdTPA/ZrO₂ were recorded (Figure 8). Both the catalysts show a very intense peak at binding energy 532 eV (Pd3p_{3/2} and O1s) as they contain PdTPA precursor and ZrO₂ as support, which is in good agreement with the well-known fact that there is direct overlap between Pd3p_{3/2} and O1s peaks [6], and cannot be assigned to confirm the presence of Pd(0).

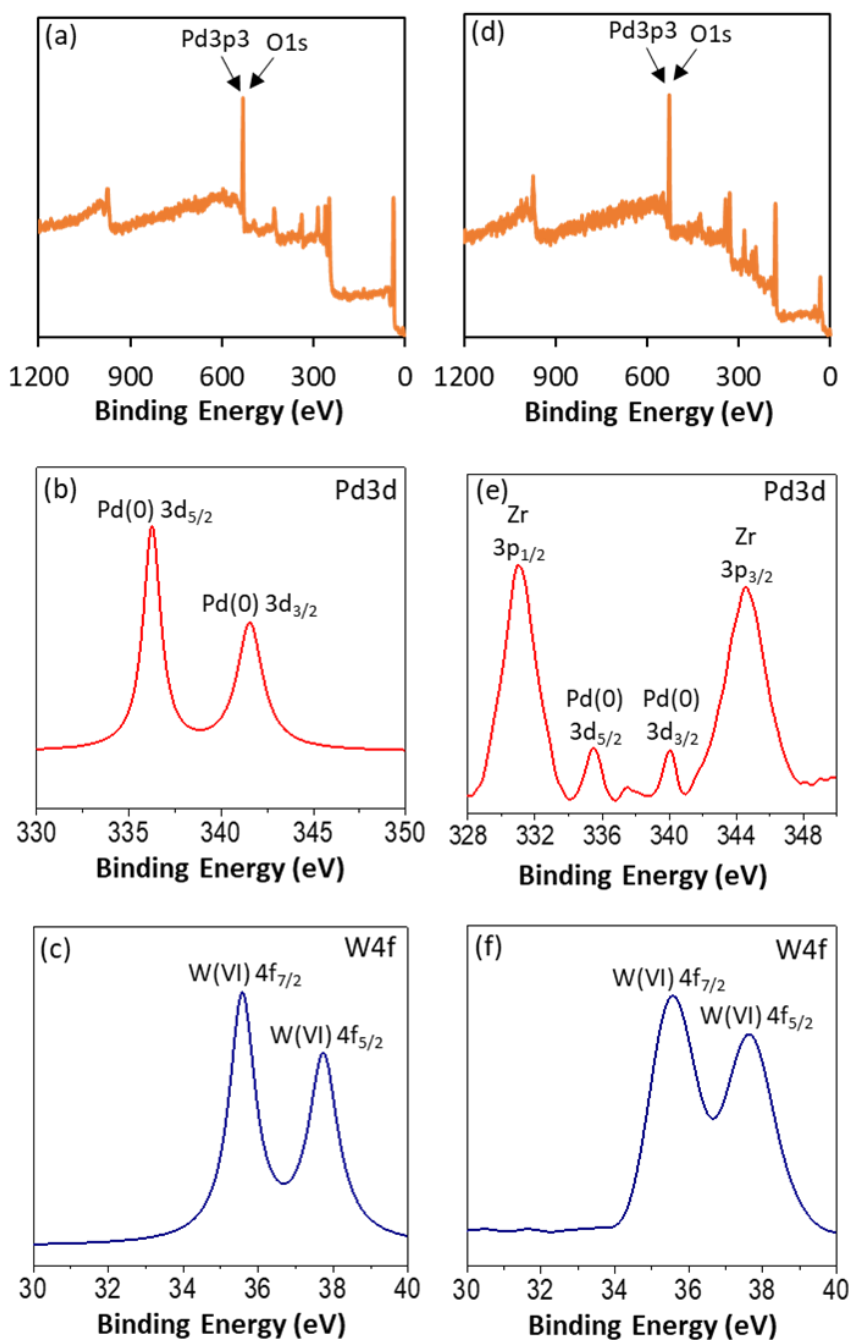


Figure 8 XPS spectra of PdTPA (a, b and c) and PdTPA/ZrO₂ (d, e and f).

Hence, we have presented instrument generated full spectra (Figure 8a & 8d) images supporting the presence of Pd(0). This was further confirmed by recording the high resolution Pd3d and W4f XPS spectra of both the materials. PdTPA shows a spin orbit doublet peak of Pd3d at binding energy 335.9 eV ($3d_{5/2}$) and 340.9 eV ($3d_{3/2}$), confirming the presence of Pd(0) [7-10]. Similarly, PdTPA/ZrO₂ reflects the same at 335.6 eV ($3d_{5/2}$) and 340.5 eV ($3d_{3/2}$), indicating the presence of the Pd(0) onto surface of ZrO₂.

The W4f peak is composed of a well resolved spin orbit doublet (35.6 eV and 37.8 eV for PdTPA, 35.6 eV and 37.7 eV for PdTPA/ZrO₂ correspond to W4f_{7/2} and W4f_{5/2}, respectively), typical of W(VI), in agreement with literature data on Keggin-type HPAs [8, 11], confirming no reduction of W(VI) during synthesis of the catalyst. Two additional high intense peaks at binding energy 331 eV and 345 eV attributed Zr3p_{3/2} and Zr3p_{1/2}, respectively [12]. XRD and XPS reveal the homogeneous dispersion of PdNCLs onto surface of ZrO₂ without alteration in Keggin structure.

TEM images of PdTPA (Figure 9a) and PdTPA/ZrO₂ (Figure 9b-9c) are presented at various magnifications. Image 9a (PdTPA) clearly shows the presence of very tiny Pd(0) nanoclusters throughout the morphology without any aggregates formation, confirming the stabilization of PdNCLs by TPA. Images 9b-9c (of PdTPA/ZrO₂) show the homogeneous dispersion of PdTPA, confirming the presence of isolatively dispersed PdNCLs onto surface of ZrO₂. For better clarification, HRTEM images (Figure 9d-9f) of PdTPA/ZrO₂ were also recorded. Images 9d & 9e clearly indicate the presence of PdNCLs of ~2 nm and less size whereas image 9f reveals the equidistance homogeneous dispersion of isolated PdNCLs onto surface of ZrO₂ without any aggregation.

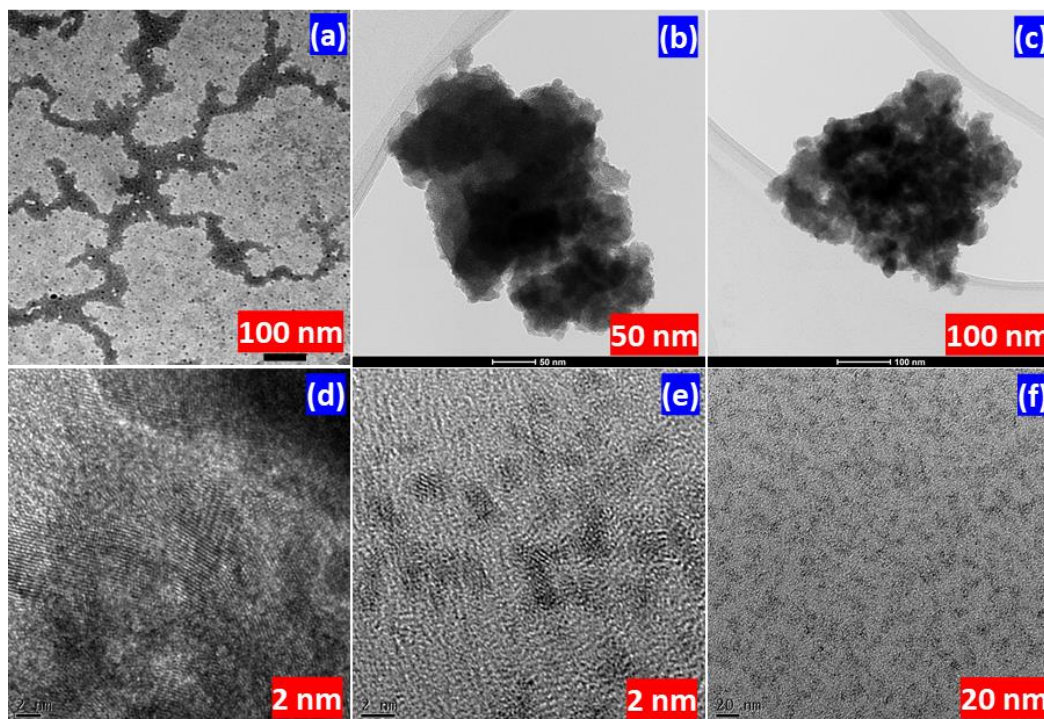


Figure 9 TEM images of PdTPA (a) and PdTPA/ZrO₂ (b & c). HRTEM images of PdTPA/ZrO₂ (d-f).

The presence of isolated PdNCLs was further confirmed by STEM (Figure 10). Images 10a and 10b highlight the isolated PdNCLs sites (dark field; as circled white spots and bright field; as black spot, respectively) with homogeneous distribution, almost having the equal nearest-neighbouring distance onto surface of zirconia. The elemental image of Pd (Figure 10i) shows that there is no cross-talks between PdNCLs. Noticeably, no aggregates formation of Pd is observed throughout the morphology. The elemental images (Figure 10c-f) show the presence of all the possible elements in the synthesized catalyst.

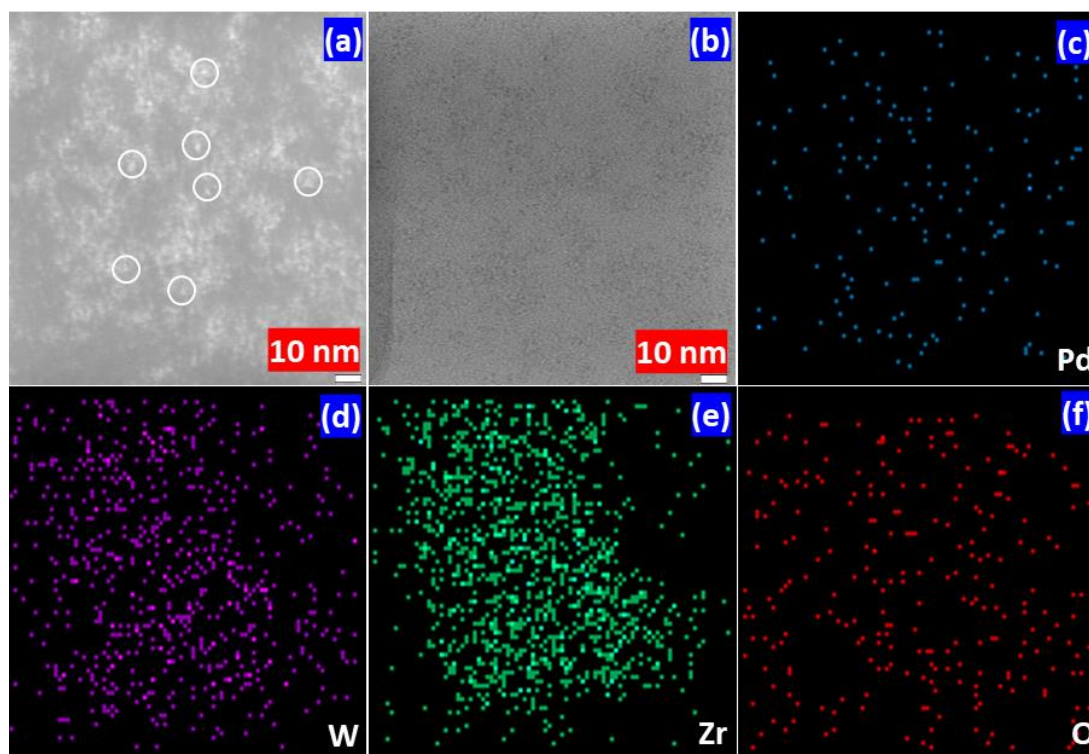


Figure 10 Dark (a) & bright (b) field STEM images and elemental images (c-f) of PdTPA/ZrO₂.

In summary, FT-IR and ³¹P MAS NMR show the presence of palladium in counter only, without degradation of TPA structure even after supporting onto ZrO₂ and a strong interaction between terminal oxygen of TPA with the hydrogen of surface hydroxyl groups of ZrO₂, respectively. The presence of Pd(0) and W(VI) are confirmed by XPS. While XRD, TEM, HRTEM and STEM confirm homogeneous dispersion of PdNCLs onto surface of ZrO₂.

Catalytic activity

SM Coupling

Iodobenzene (1.96 mmol) and phenylboronic acid (2.94 mmol) were selected as the test substrates and effect of different reaction parameters (Figure 11) such as palladium concentration, time, temperature, base, solvent and solvent ratio were studied to optimize the conditions for maximum conversion.

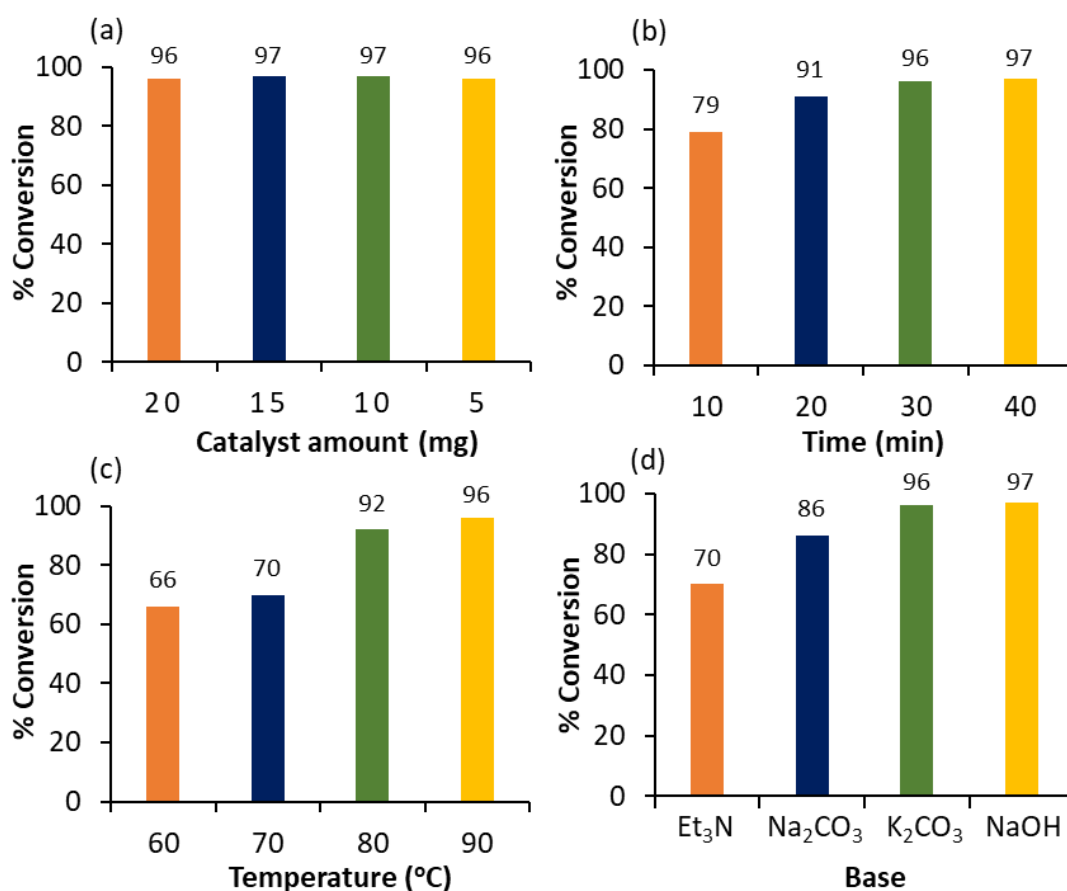


Figure 11 Optimization of SM coupling. Reaction conditions: (a) Effect of catalyst amount- K₂CO₃ (3.92 mmol), EtOH: H₂O (3:7 mL), time (30 min), temperature (90 °C); (b) Effect of time- catalyst (5 mg), K₂CO₃ (3.92 mmol), EtOH: H₂O (3:7 mL), temperature (90 °C); (c) Effect of temperature- catalyst (5 mg), K₂CO₃ (3.92 mmol), EtOH: H₂O (3:7 mL), time (30 min); (d) Effect of base- catalyst (5 mg), base (3.92 mmol), EtOH: H₂O (3:7 mL), time (30 min), temperature (90 °C).

Initially, the effect of palladium concentration was studied by varying the catalyst amount from 20 mg to 5 mg (1.41×10^{-3} mM to 3.52×10^{-4} mM Pd concentration) and results are shown in figure 11a. It can be seen that with decrease in catalyst amount the % conversion remains unaltered. Obtained results show that very low concentration of Pd (1.06×10^{-3} mM) is sufficient to achieve 96 % conversion.

The influence of time on catalytic conversion was screened between 10 min to 40 min as shown in figure 11b. Initially, ≈ 1.22 -fold % conversion increase is observed from 10 to 30 min. On further, prolonging the reaction (40 min), no significant effect on reaction conversion was observed. Hence, 30 min was optimized for the reaction.

The effect of temperature was assessed between 60 to 90 °C and obtained results are presented in figure 11c. It shows that % conversion increases with increase in temperature as expected. Here, ≈ 1.45 -fold % conversion increase is obtained from 60 to 90 °C. Hence, sufficient activation energy was achieved at 90 °C and hence considered as optimum temperature for the maximum % conversion.

Effect of various bases was also studied and obtained results are presented in figure 11d. The study indicates that organic base triethyl amine (Et_3N), is less favorable for coupling reaction compared to that of inorganic bases. The highest conversion was found in case of K_2CO_3 and NaOH . As K_2CO_3 is environmentally benign, easy to handle and non-hygroscopic in nature compared to NaOH , further study was carried out with K_2CO_3 .

The effect of different solvents on the reaction is tabulated in table 1. Obtained results show that maximum % conversion was obtained in case of ethanol compared to toluene and acetonitrile. This is in good agreement with the reported one [13-15] , stating that polar solvents tend to give the best result for coupling reactions. The low % conversion in water may be due to the lower solubility of substrates compared to ethanol. Hence, ethanol was selected as an appropriate solvent for further study.

Table 1 Effect of solvent

Solvent	% Conversion
Toluene	2
Acetonitrile	5
Ethanol	60
H ₂ O	36

Reaction conditions: Catalyst (5 mg), K₂CO₃ (3.92 mmol), solvent (10 mL), time (30 min), temperature (90 °C).

Finally, the effect of solvent to water (Ethanol: H₂O) ratio was studied and obtained results are presented in table 2.

Table 2 Effect of solvent ratio

Ethanol: H ₂ O	% Conversion
1:9	69
2:8	84
3:7	96
4:6	97
5:5	97

Reaction conditions: Catalyst (5 mg), K₂CO₃ (3.92 mmol), time (30 min), temperature (90 °C).

Obtained results show that initially, with increase in ethanol amount the % conversion increases, this may be due to the increase in solubility of substrates in ethanol. This trend is found from ratio (1:9) mL to (3:7) mL. For higher ratio (4:6) to (5:5) mL, no significant change in % conversion is observed. Maximum 96 % conversion is achieved for (3:7) mL.

From the above study, the optimized conditions for the maximum % conversion (96) are: iodobenzene (1.96 mmol), phenylboronic acid (2.94 mmol), K_2CO_3 (3.92 mmol), conc. of Pd (3.76×10^{-4} mmol, 0.0192 mol%), substrate/catalyst ratio (5215/1), C_2H_5OH : H_2O (3:7 mL), 30 min, 90 °C. The calculated TON is 5006 and TOF is 10012 h^{-1} .

Heck coupling

In this case, iodobenzene (0.98 mmol) and styrene (1.47 mmol) were selected as the test substrates. Effect of different reaction parameters such as palladium concentration, time, temperature, base, solvent and solvent ratio was studied to optimize the conditions for maximum conversion. Obtained results are shown in respective figures (Figure 12).

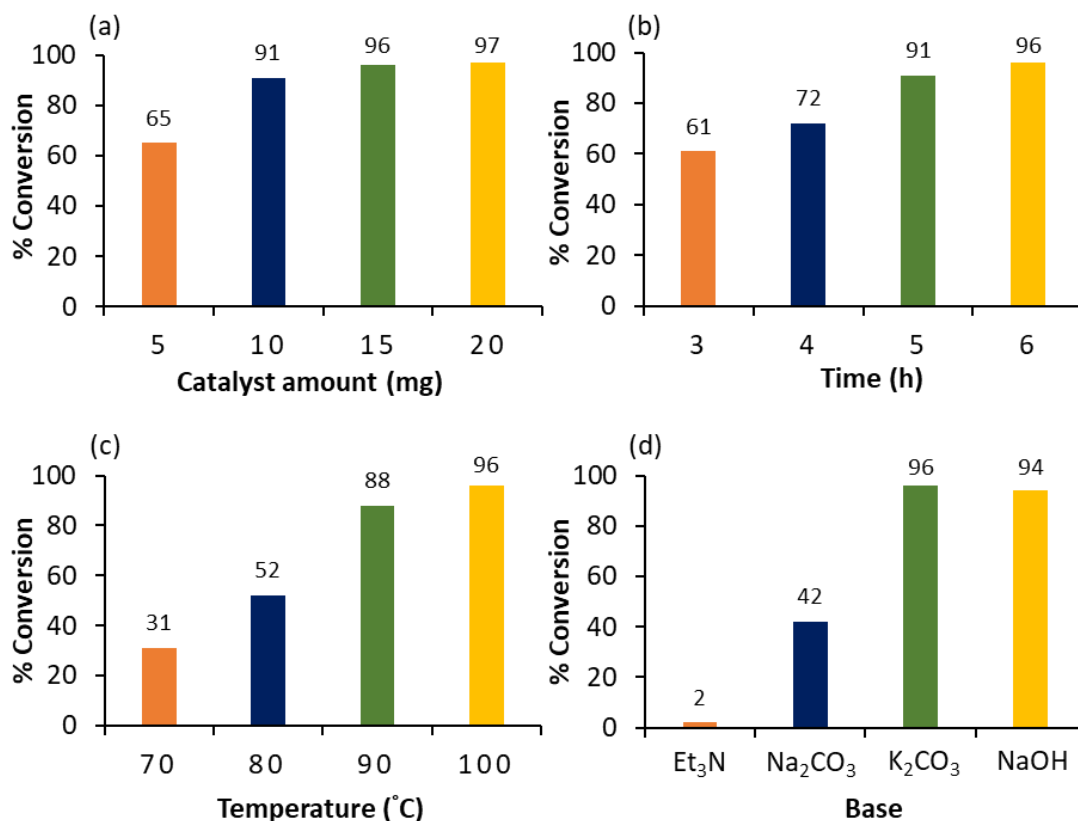


Figure 12 Optimization of Heck coupling. Reaction conditions: (a) Effect of catalyst amount- K₂CO₃ (1.96 mmol), DMF:H₂O (3:2 mL), time (6 h), temperature (100 °C); (b) Effect of time- catalyst (15 mg), K₂CO₃ (1.96 mmol), DMF:H₂O (3:2 mL), temperature (100 °C); (c) Effect of temperature- catalyst (15 mg), K₂CO₃ (1.96 mmol), DMF:H₂O (3:2 mL), time (6 h); (d) Effect of base- catalyst (15 mg), base (1.96 mmol), DMF:H₂O (3:2 mL), time (6 h), temperature (100 °C).

It should be noted that the explanation will remain the same as given in the section of SM coupling.

The effect of different solvents was studied and obtained results are shown in table 3. Study indicates that maximum % conversion was obtained in case of DMF compared to toluene and ethanol. This is in good agreement with the reported one [13-15] , stating that polar, aprotic solvents tend to give the best results for Heck coupling. Low % conversion is observed in case of water which may be due to the lower solubility of substrate. Hence, DMF was selected as an appropriate solvent for further study.

Table 3 Effect of solvent

Solvent	% Conversion
Toluene	6
Ethanol	32
DMF	56
H ₂ O	2

Reaction conditions: Catalyst (15 mg), K₂CO₃ (1.96 mmol), time (6 h), temperature (100 °C).

Finally, the effect of solvent to water (DMF: H₂O) ratio was assessed and data are tabulated in table 4.

Table 4 Effect of solvent ratio

DMF: H ₂ O	% Conversion
1:4	25
2:3	64
3:2	96
4:1	78

Reaction conditions: Catalyst (15 mg), K₂CO₃ (1.96 mmol), time (6 h), temperature (100 °C).

Obtained results show that initially, with increase in DMF amount the % conversion increases, this may be due to better solubility of substrates in DMF. This trend was found from ratio (1:4) mL to (3:2) mL. For higher ratio (4:1) mL, % conversion decreases, because of incomplete solubility of base in 1 mL of water. Maximum, 96 % conversion was achieved for (3:2) mL.

The optimized conditions for the maximum % conversion (96) are: iodobenzene (0.98 mmol), styrene (1.47 mmol), K₂CO₃ (1.96 mmol), conc. of Pd (1.13×10^{-3} mmol, 0.115 mol%), substrate/catalyst ratio (869/1), DMF:H₂O (3:2 mL), time (6 h), temperature (100 °C). The calculated TON is 834 and TOF is 139 h⁻¹.

Hydrogenation

To evaluate the efficiency of the catalyst for hydrogenation, cyclohexene (9.87 mmol) was selected as the test substrate. Effect of different reaction parameters such as palladium concentration, time, temperature, pressure and solvent were studied to optimize the conditions for maximum conversion (Figure 13).

The effect of Pd concentration (Figure 13a) was assessed by varying the catalyst amount from 10 to 25 mg (substrate/catalyst ratio from 13130/1 to 5251/1, respectively). Initially, with increase in catalyst amount from 10 to 20 mg, % conversion also increases. A higher concentration of Pd would mean a higher number of Pd sites to tolerate the substrate and give higher conversion. With further increasing Pd concentration, no significant change in % conversion was observed. 20 mg of the catalyst was found to be sufficient for the highest conversion (94 %).

Temperature influence was studied between 60 to 90 °C and obtained results are shown in figure 13b. Results show, ≈ 1.52 -fold increase in % conversion with rise in temperature from 60 to 80 °C, as expected. Further increase in the temperature show backward proceeding of the reaction. The sufficient activation energy was achieved by 80 °C for maximum conversion.

The influence of H₂ pressure was evaluated by varying the pressure from 7 to 10 bar (Figure 13c). Increase in pressure from 7 to 10 bar, resulted in ≈ 1.47 -fold increase in % conversion. Hence, the reaction followed first order with respect to H₂ pressure. Keeping in mind the green chemistry principle, we did not proceed further for effect of higher H₂ pressure. Maximum, 94 % conversion was achieved at 10 bar H₂ pressure.

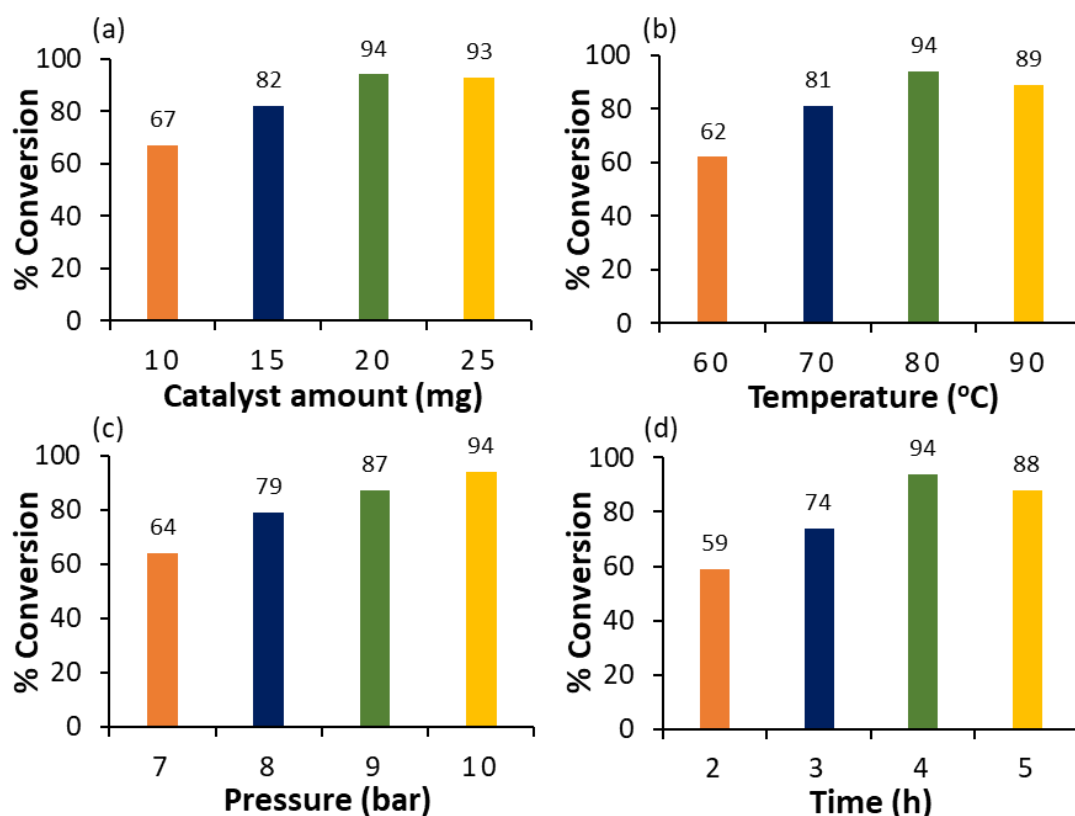


Figure 13 Optimization of reaction parameters. Reaction conditions: (a) Effect of catalyst amount- cyclohexene (9.87 mmol), H₂O (50 mL), temperature (80 °C), H₂ pressure (10 bar), time (4 h); (b) Effect of temperature- cyclohexene (9.87 mmol), catalyst (20 mg), H₂O (50 mL), H₂ pressure (10 bar), time (4 h); (c) Effect of pressure- cyclohexene (9.87 mmol), catalyst (20 mg), H₂O (50 mL), temperature (80 °C), time (4 h); (d) Effect of time- cyclohexene (9.87 mmol), catalyst (20 mg), H₂O (50 mL), temperature (80 °C), H₂ pressure (10 bar).

The effect of time was screened by varying the reaction time from 2 h to 5 h (Figure 13d). Obtained results show that with increase in time up to 4 h, the % conversion also increases, which is in good agreement with the well-known fact that as time increases, the formation of reactive intermediates from the reactant increases, and finally converted into the products. On further prolonging the reaction up to 5 h, the % conversion decreases. Hence, 4 h was optimized for the maximum % conversion.

Effect of various solvents was evaluated and found results are tabulated in table 5. Comparatively, high % conversion was achieved in EtOH: H₂O and IPA: H₂O solvent mixture, whereas moderate conversion was obtained in ACN: H₂O system due to the following proton transfer nature of the solvents: EtOH > IPA > ACN. However, it was miracle that higher % conversion was obtained under the identical reaction conditions for neat water as a solvent (i.e. 94 %). Hence, to make the present system environmentally benign, water was optimized as a solvent for further study.

Table 5 Effect of solvent

Solvent (20: 30) mL	% Conversion
CH ₃ CN: H ₂ O	79
IPA: H ₂ O	89
EtOH: H ₂ O	96
H ₂ O (50) mL	94

Reaction condition: Catalyst (20 mg), temperature (80 °C), H₂ pressure (10 bar), time (4 h).

The optimized conditions for the maximum % conversion (94) are: Cyclohexene (9.87 mmol), H₂O (50 mL), conc. of Pd (1.50×10^{-3} mmol, 0.015 mol%), substrate/catalyst ratio (6565/1), time (4 h), temperature (80 °C). The calculated TON is 6171 and TOF is 1543 h⁻¹.

Control Experiments

In all the three reactions, control experiments were carried out with TPA, ZrO₂, PdCl₂ and PdTPA under optimized conditions in order to understand the role of each component and results are shown in table 6. It is seen from the table that TPA and ZrO₂ were inactive towards the reactions. Almost same conversion was found in the case of PdCl₂, PdTPA and PdTPA/ZrO₂ in all

reactions. This indicates that Pd is real active species responsible for the reactions and we could succeed in supporting the same without any alteration in activity.

Table 6 Control experiment

Catalyst	SM	Heck	Hydrogenation
	% Conversion ^a	% Conversion ^b	% Conversion ^c
TPA (^a 1.15, ^b 3.46, ^c 4.62 mg)	N. R.	N. R.	N. R.
ZrO ₂ (^a 3.85, ^b 11.54, ^c 15.38 mg)	N. R.	N. R.	N. R.
PdCl ₂	99	96	93
PdTPA	96	96	91
PdTPA/ZrO ₂	96	96	94

Reaction conditions. (a) *SM coupling*: iodobenzene (1.96 mmol), phenylboronic acid (2.94 mmol), catalyst (0.04 mg Pd, 0.0192 mol% Pd), K₂CO₃ (3.92 mmol), C₂H₅OH: H₂O (3:7 mL), time (30 min), temperature (90 °C); (b) *Heck coupling*: iodobenzene (0.98 mmol), styrene (1.47 mmol), catalyst (0.12 mg Pd, 0.115 mol% Pd), K₂CO₃ (1.96 mmol), DMF: H₂O (3:2 mL), time (6 h), temperature (100 °C); (c) *Hydrogenation*: cyclohexene (9.87 mmol), catalyst (0.16 mg Pd, 0.015 mol% Pd), H₂O (50 mL), time (4 h), temperature (80 °C), H₂ pressure (10 bar). N. R. – No reaction.

Leaching and Heterogeneity test

The leaching of PdNCLs from the support was investigated in all reactions by centrifuging the catalyst in between the reactions while, the leaching of TPA from ZrO₂ was checked after completion of the reactions by treating the aqueous layer with 10 % ascorbic acid solution and absence of blue colour indicated no leaching of TPA. In case of SM coupling, reaction was carried out for 10 min, centrifuged and then filtrate was allowed to react up to 30 min. Similarly, in case of Heck coupling, reaction was carried out for 3 h, centrifuged and then filtrate was allowed to react up to 6 h. Whereas, in case of

hydrogenation, reaction was carried out for 2 h, centrifuged and then filtrate was allowed to react up to 4 h. After that obtained reaction mixtures were extracted by using dichloromethane and analyzed by Gas chromatogram. In all the cases, obtained results (Table 7) show that there was no significant change in % conversion of the reaction after removing the catalyst, indicating the absence of active species in the reaction mixture which proves that there was no leaching of PdNCLs during the reactions.

Table 7 Leaching test

Catalyst	SM	Heck	Hydrogenation
	% Conversion ^a	% Conversion ^b	% Conversion ^c
PdTPA/ZrO ₂	79 (after 10 min)	61 (after 3 h)	59 (after 2 h)
	80 (after 30 min)	62 (after 6 h)	60 (after 4 h)

Reaction conditions. (a) *SM coupling*: iodobenzene (1.96 mmol), phenylboronic acid (2.94 mmol), catalyst (0.04 mg Pd, 0.0192 mol% Pd), K₂CO₃ (3.92 mmol), C₂H₅OH: H₂O (3:7 mL), temperature (90 °C); (b) *Heck coupling*: iodobenzene (0.98 mmol), styrene (1.47 mmol), catalyst (0.12 mg Pd, 0.115 mol% Pd), K₂CO₃ (1.96 mmol), DMF: H₂O (3:2 mL), temperature (100 °C); (c) *Hydrogenation*: cyclohexene (9.87 mmol), catalyst (0.16 mg Pd, 0.015 mol% Pd), H₂O (50 mL), temperature (80 °C), H₂ pressure (10 bar).

However, minor change in % conversion may be due to the instrument error (\pm 1-1.5 %). In addition, product mixture was also analyzed by AAS, and obtained results were below its detection limit indicating no emission of Pd into the reaction mixture. This study confirms neither leaching of Pd nor TPA, indicating the strong interaction between ZrO₂ and PdTPA, which does not allow it to leach into the reaction mixture. Here, withholding of active species onto support during the reaction shows that present catalyst is of category C [16] and truly heterogeneous in nature.

Recyclability and sustainability of the catalyst

Sustainability of the catalyst is the key challenge for any process, and for the same recycling test was studied for PdTPA and PdTPA/ ZrO_2 (Figure 14). In order to regenerate the catalyst, after reaction completion, the catalyst was centrifuged, washed with dichloromethane followed by consequent washes with distilled water and finally dried at 100 °C for an hour to reuse it for next catalytic run.

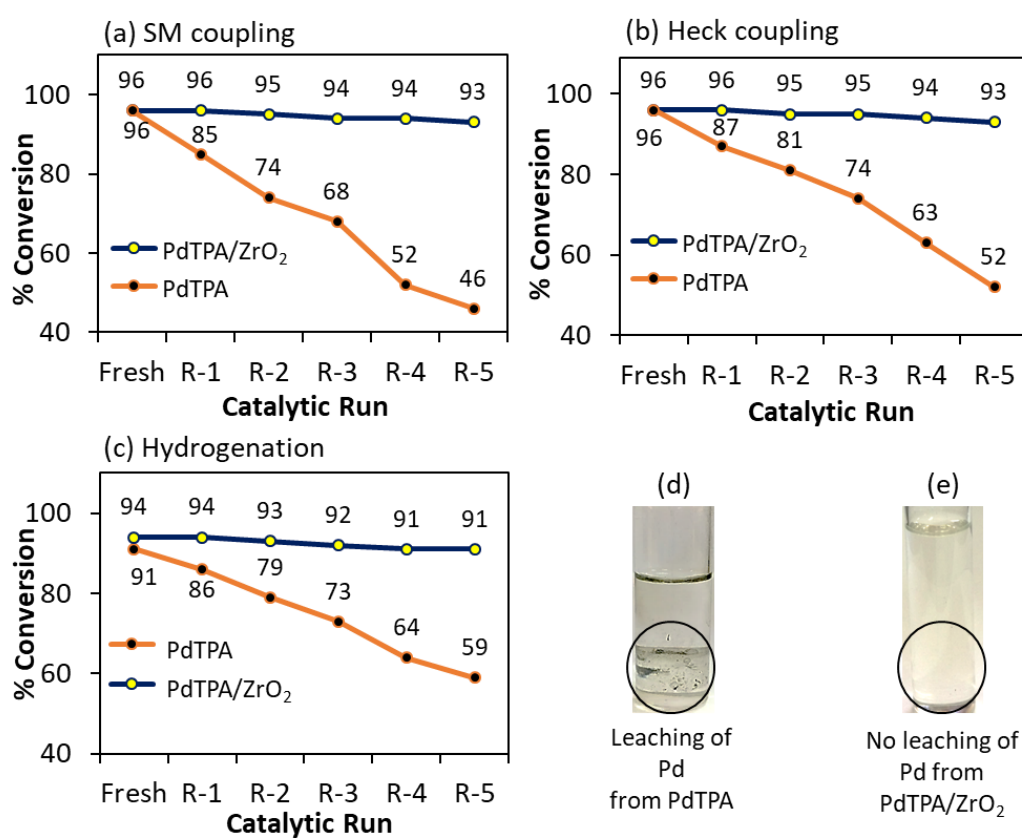


Figure 14 Recycling test. Reaction conditions: (a) *SM coupling*- catalyst (0.04 mg Pd, 0.0192 mol% Pd), K_2CO_3 (3.92 mmol), $\text{C}_2\text{H}_5\text{OH}$: H_2O (3:7 mL), time (30 min), temperature (90 °C); (b) *Heck coupling*- catalyst (0.12 mg Pd, 0.115 mol% Pd), K_2CO_3 (1.96 mmol), DMF: H_2O (3:2 mL), time (6 h), temperature (100 °C); (c) *Hydrogenation*- catalyst (0.16 mg Pd, 0.015 mol% Pd), H_2O (50 mL), time (4 h), temperature (80 °C), H_2 pressure (10 bar); (d) Leaching of Pd from PdTPA during the reaction and (e) No leaching of Pd from PTPA/ ZrO_2 during the reaction.

Obtained results show the gradual decrease in the % conversion in case of PdTPA during all the reactions, confirming the leaching of active species PdNCLs (Figure 14d). In contrast, PdTPA/ZrO₂ did not show any appreciable change in the % conversion up to five cycles for all reactions, indicating that the catalyst was stable, and can be regenerated and reused for further catalytic runs also. Here, ZrO₂ plays an important role by supporting PdTPA over its surface via strong interaction for the sustainability of catalyst activity.

Characterization of regenerated catalyst

In order to check the stability, the regenerated catalyst was characterized by EDS, FT-IR, XRD, BET and XPS.

EDS values of Pd (0.78 wt%) and W (17.14 wt%) of regenerated PdTPA/ZrO₂ (Figure 15) is in good agreement with values of fresh catalyst (0.80 wt% of Pd, 17.36 wt% of W) confirming no emission of Pd as well as TPA from ZrO₂ during the reaction.

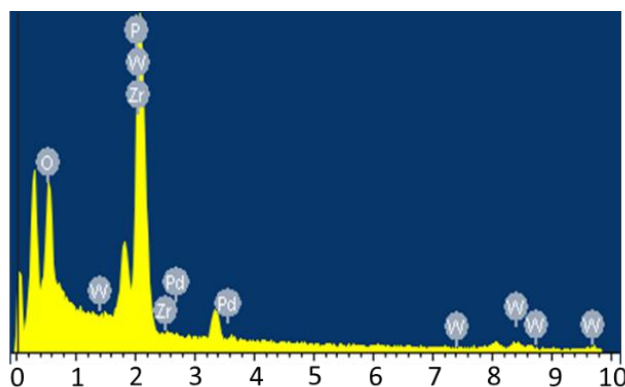


Figure 15 EDX mapping of regenerated PdTPA/ZrO₂.

The FT-IR spectra of the fresh and regenerated catalyst are shown in figure 16. From the spectra it can be seen that almost identical spectra was obtained without any significant shift in characteristic bands of regenerated catalyst compared to fresh catalyst, indicating that catalyst structure remained unaltered even after the regeneration. However, the spectrum was slightly

different in terms of intensity. This might be due to the sticking of the substrates on the surface, although this might not be significant in the reutilization of the catalyst [17].

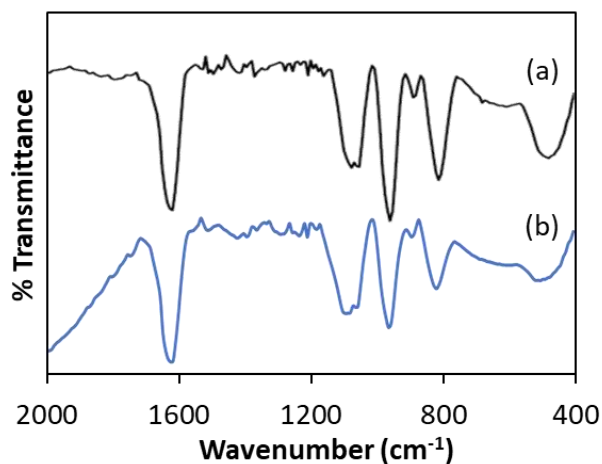


Figure 16 FT-IR spectra of (a) PdTPA/ZrO₂ and (b) R- PdTPA/ZrO₂.

XRD patterns of fresh and regenerated catalyst are shown in figure 17. Obtained results revealed the retention of highly dispersed nature of the catalyst. Absence of any characteristic peaks regarding Pd aggregates as well as TPA clearly indicates the sustainability of the catalyst during the reaction.

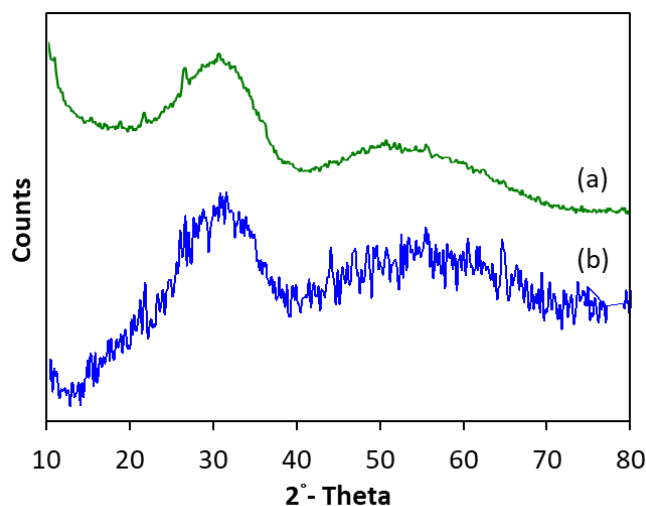


Figure 17 XRD patterns of (a) PdTPA/ZrO₂ and (b) R- PdTPA/ZrO₂.

Almost same BET surface area of fresh ($202 \text{ m}^2/\text{g}$) and regenerated ($198 \text{ m}^2/\text{g}$) catalysts indicated that PdNCLs sites remains intact during the reaction, do not undergo sintering or aggregation. Moreover, no change in N_2 sorption isotherms (Figure 18) of regenerated one proved that surface phenomena as well as bulk remains intact.

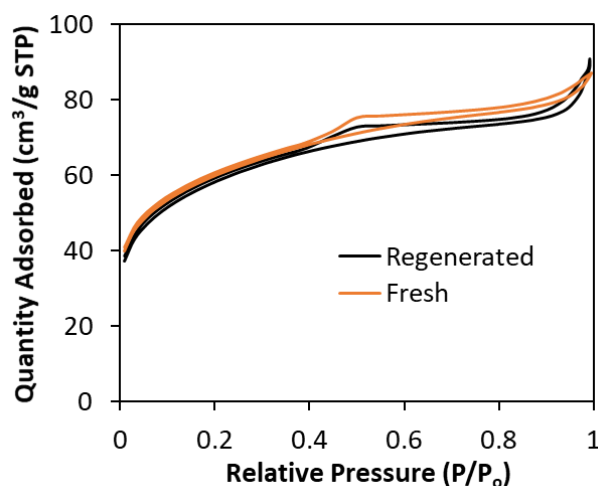


Figure 18 N_2 sorption isotherms of fresh and regenerated catalysts.

XPS spectra of regenerated PdTPA/ ZrO_2 is displayed in figure 19. The spectrum of regenerated catalyst was found to be identical with fresh one (Figure 8), confirmed the retention of Pd active species as well as W(VI), which did not undergo reduction during the reaction, indicating the sustainability of the catalyst.

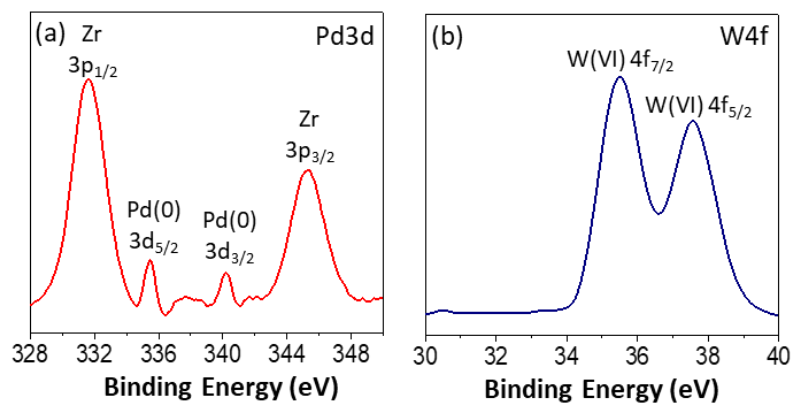
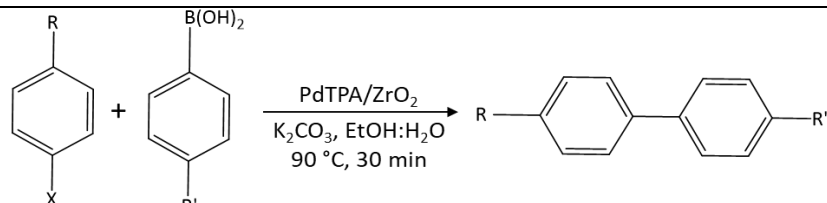
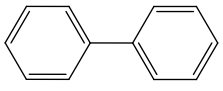
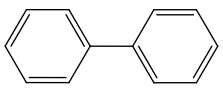
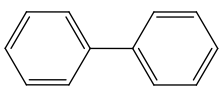
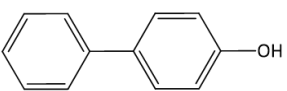
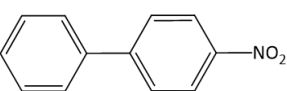
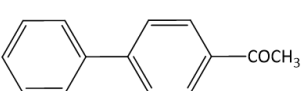


Figure 19 XPS spectra of regenerated catalyst (a) Pd3d and (b) W4f.

Viability of the catalyst

Under the optimized condition, the scope and limitations of substrates for SM coupling were investigated by using different halobenzenes and phenylboronic acid (Table 8).

Table 8 Substrate study for SM coupling

					
R	X	R'	Product	% Conversion	TON/TOF (h ⁻¹)
H	I	H		96	5006/10012
H	Br	H		60 92 (5 h)	3129/6258 4797/959
H	Cl	H		5 85 (10 h)	261/522 4432/443
OH	Br	H		94	4902/9804
NO ₂	Br	H		97	5058/10116
COCH ₃	Br	H		89	4641/9282

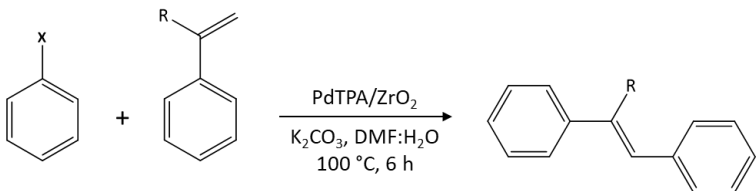
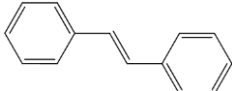
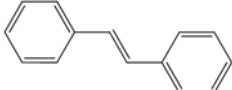
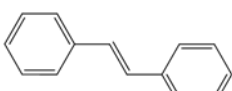
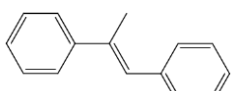
Reaction conditions: Halobenzene (1.96 mmol), Phenylboronic acid (2.94 mmol), K₂CO₃ (3.92 mmol), conc. of Pd (0.0192 mol%), substrate/catalyst ratio (5215/1), C₂H₅OH:H₂O (3:7 ml), time (30 min), temperature (90 °C).

Coupling of iodobenzene with phenylboronic acid gave higher conversion compared to bromobenzene and chlorobenzene as expected. The found reactivity order was Ph-I > Ph-Br > Ph-Cl. However, in case of bromobenzene and chlorobenzene higher % conversion was achieved by prolonging the reaction for 10 h. Presence of strongly electron donating group like -OH is less

favorable for the coupling reaction, though in the case of p-bromophenol, high conversion was obtained. This may be due to the complete solubility of the substrate in reaction medium at optimized temperature which facilitates the reaction. This indicates the conversion of the reaction may be greatly dependent on halobenzene substrate. Substituted bromobenzene with strongly electron withdrawing group such as $-\text{NO}_2$ facilitates the reaction, and hence p-bromonitrobenzene gave the 97 % conversion. Similarly, p-bromoacetophenone gave high % conversion due to the presence of moderate electron withdrawing group $-\text{COCH}_3$.

Similarly, under optimized conditions, scope and limitations of substrates for Heck coupling were investigated by using different halobenzenes and styrene derivatives (Table 9).

Table 9 Substrate study for Heck coupling

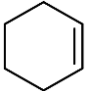
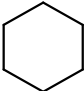
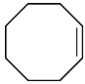
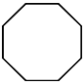
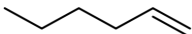
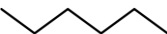
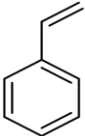
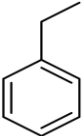
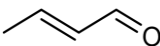
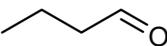
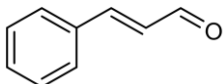
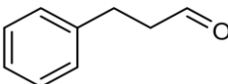
				
X	R	Product	% Conversion	TON/TOF (h ⁻¹)
I	H		96	834/139
Br	H		66 95 (10 h)	574/96 826/83
Cl	H		7 44 (10 h)	61/10 382/38
I	CH ₃		66 84 (10 h)	574/96 730/73

Reaction conditions: Halobenzene (0.98 mmol), styrene (1.47 mmol), K₂CO₃ (1.96 mmol), Conc. of Pd (0.115 mol%), substrate/catalyst ratio (869/1), DMF: H₂O (3:2 mL), time (6 h), temperature (100 °C).

Coupling of iodobenzene with styrene gave higher conversion compare to bromobenzene and chlorobenzene. The found reactivity order was Ph-I > Ph-Br > Ph-Cl. However, in case of bromobenzene and chlorobenzene higher % conversion was achieved by increasing the catalyst amount. Coupling of iodobenzene with α -methyl styrene (66 %) was lower compared to the coupling of iodobenzene with styrene (96 %). This may be due to crowding effect of the methyl group.

For hydrogenation, the efficiency of the catalyst was evaluated towards different aliphatic and aromatic alkenes. Obtained results (Table 10) shows that, even though all substrates are insoluble in water, present catalyst is highly viable. Ring size effect was observed for the activity of the catalyst. Moreover, the catalyst was found to be active for selective hydrogenation of the C=C bond without tolerating the C=O bond when simultaneously present in the substrates.

Table 10 Substrate study for hydrogenation

Substrate	Product	% Conversion/Selectivity	TON/TOF
		94	6171/1543
		61	4005/1001
		76	4989/1247
		92	6040/1510
		82/100	5383/1346
		69/100	4530/1133

Reaction conditions: Substrate (9.87 mmol), conc. of Pd (0.015 mol%), substrate/catalyst ratio (6565/1), H₂O (50 mL), temperature (80 °C), H₂ pressure (10 bar), time (4 h).

Comparison with reported catalyst

Catalytic activity of the present catalyst is also compared with reported catalysts for C-C coupling reactions (Table 11 & 12) in terms of iodobenzene and hydrogenation reaction (Table 13) in terms of cyclohexene as one of the substrates.

It is seen for SM coupling (Table 11), that the present catalyst is superior in terms of mol% of Pd as well as reaction time as compared to all reported catalytic systems.

Table 11 Comparison of catalytic activity for SM coupling with reported catalyst in organic-water solvent mixture with respect to iodobenzene

Catalyst	Active amount of Pd (mol %)	Solvent	Temp. (°C)/Time (h)	% Conversion/TON /TOF (h ⁻¹)
Pd-ScBTC NMOFs [18]	0.5	C ₂ H ₅ OH: H ₂ O (1:1 mL)	40/0.5	99/194/388
Pd/C [19]	0.37	C ₂ H ₅ OH: H ₂ O (1:1 mL)	40/0.5	99/268/535
Oximepalladacycle catalyst [20]	0.3	C ₂ H ₅ OH: H ₂ O (1:1 mL)	RT/0.3	95/317/1057
Fe ₃ O ₄ /Ethyl-CN/Pd [21]	0.2	C ₂ H ₅ OH: H ₂ O (1:1 mL)	RT/0.2	98/49/245
G-BI-Pd [22]	0.45	C ₂ H ₅ OH: H ₂ O (1:1 mL)	80/0.084	98/219/2613
PdTPA/ZrO₂ (Present catalyst)	0.0192	C₂H₅OH: H₂O (3:7 mL)	90/0.5	96/5006/10012

In case of Heck coupling (Table 12), Shabbani and his co-worker [23] reported the reaction using universal green solvent water with moderate reaction conversion and low TON/TOF compare to the present report. Guo et al. [24], Patil et al. [25], Sajiki et al. [26] and Zekri et al. [27] have reported the reaction using neat organic solvent only with consumption of high mol% of Pd as active

species as well as comparatively lower % conversion. Here, the uniqueness of the present catalyst lies in terms of the used reaction medium, water-organic solvent mixture (DMF: H₂O), lower mol% of Pd, high % conversion as well as high TON/TOF.

Table 12 Comparison of catalytic activity for Heck reaction with reported catalysts with respect to iodobenzene

Catalyst	Active amount of Pd (mol %)	Solvent	Temp. (°C)/Time (h)	% Conversion/TON /TOF (h ⁻¹)
PdTSPc@KP-GO [23]	0.792	H ₂ O (10 mL)	reflux/9	89/111/12
Pd/CNCs [24]	1.412	DMF (10 mL)	40/5	93/65/13
NO ₂ -NHC-Pd@Fe ₃ O ₄ [25]	1.0	CH ₃ CN (5 mL)	80/5	96/96/19
5% Pd/CM [26]	0.2	DMA	80/24	61/3050/127
PF ₆ -Pd [27]	1.7	DMF (3 mL)	120/6	95/56/9
PdTPA/ZrO₂ (Present catalyst)	0.115	DMF: H₂O (3:2 mL)	100/6	96/834/139

In case of hydrogenation, the true competence of the presented catalyst is also compared with reported systems (Table 13). Liu et al. [28] reported high conversion at a lower temperature, with the utilization of very high H₂ pressure (20 bar) for the reaction compared to present work. Zhang et al. [29] reported the reaction at 35 °C with very poor conversion, moreover a mole % of catalyst was too high. Leng et al. [30] achieved high conversion using formic acid as an *in-situ* proton transferring agent with a very high concentration of the Pd compared to the present catalytic system along with very low TON. Panpranot et al. [31] achieved excellent conversion using supercritical CO₂ as a

solvent at 60 bar pressure (extremely high condition). Enumerated data of table 13 indicates that the present catalytic system is best one of all reported one in terms of activity under mild reaction conditions.

Table 13 Comparison with the reported catalyst with respect to cyclohexene hydrogenation

Catalyst	Active amount of Pd (mol%)	Solvent	Temp. (°C)	Pressure (bar)	% Conv./TON/TOF
SH-IL-1.0wt%Pd [28]	0.02	Auto-clave	60	20	99/5000/5000
Pd/MSS@ZIF-8 [29]	0.1738	Ethyl acetate	35	1	5.6/560/93
Pd@CN [30]	2.208	Formic acid	90	(Proton transfer)	96/44/3.67
Pd/SiO ₂ [31]	0.091	CO ₂ (60 bar)	25	10	96/1097/6582
PdTPA/ZrO₂ (Present catalyst)	0.015	Water	80	10	94/6171/1543

It is interesting to note that no report was found in which the same catalyst has been applied for both the C-C coupling as well hydrogenation reactions with respect to iodobenzene and cyclohexene as one of the substrates, respectively. The present catalyst is superior in terms of used concentration of Pd, reaction time as well as TON/TOF in all three reactions. Its high activity compared to reported catalytic systems, may be due to the high efficiency of the PdNCLs.

Conclusion

- Synthesis of true heterogeneous catalyst, Zirconia supported stabilized PdNCLs by 12-tungstophosphoric acid (PdTPA/ZrO₂), is carried out successfully by impregnation and post reduction method
- FT-IR, ³¹P MAS NMR and XRD show the retention of Keggin structure, XPS reveals the oxidation states of Pd(0) and W(VI), whereas TEM, HRTEM and STEM confirm the presence of PdNCLs in the synthesized catalyst
- The present catalyst depicts outstanding activity for C-C coupling (SM and Heck) and hydrogenation (% conversion: 96, 96, 94; TON: 5006, 834, 6171, respectively)
- The catalyst is regenerated and recycled successfully up to five cycles (and can be used for more) without significant loss in catalytic activity. EDX, FT-IR, XRD, BET and XPS of regenerated catalyst confirm the sustainability of the catalyst
- Substrate study shows that catalyst is highly viable towards various functionalities as well as depicts superior catalytic activity compared to those of reported systems

References

- [1] N. Mizuno, J. S. Min and A. Taguchi, *Chem. Mater.*, 16, 2819-2825, (2004).
- [2] I. Kozhevnikov, K. Kloetstra, A. Sinnema, H. Zandbergen and H. v. van Bekkum, *J. Mol. Catal. A: Chem.*, 114, 287-298, (1996).
- [3] T. Okuhara, N. Mizuno and M. Misono, *Appl. Catal., A*, 222, 63-77, (2001).
- [4] C. Bianchini, D. G. Burnaby, J. Evans, P. Frediani, A. Meli, W. Oberhauser, R. Psaro, L. Sordelli and F. Vizza, *J. Am. Chem. Soc.*, 121, 5961-5971, (1999).
- [5] A. Patel and S. Singh, *Microporous Mesoporous Mater.*, 195, 240-249, (2014).
- [6] A. V. Matveev, V. V. Kaichev, A. A. Saraev, V. V. Gorodetskii, A. Knop-Gericke, V. I. Bukhtiyarov and B. E. Nieuwenhuys, *Catal. Today*, 244, 29-35, (2015).
- [7] Y. Leng, C. Zhang, B. Liu, M. Liu, P. Jiang and S. Dai, *ChemSusChem*, 11, 3396-3401, (2018).
- [8] R. Villanneau, A. Roucoux, P. Beaunier, D. Brouri and A. Proust, *RSC Adv.*, 4, 26491-26498, (2014).
- [9] L. D'Souza, M. Noeske, R. M. Richards and U. Kortz, *Appl. Catal., A*, 453, 262-271, (2013).
- [10] L. D'Souza, M. Noeske, R. M. Richards and U. Kortz, *J. Colloid Interface Sci.*, 394, 157-165, (2013).
- [11] S. Rana and K. M. Parida, *Catal. Sci. Technol.*, 2, 979-986, (2012).
- [12] Y. Zhu, W. D. Wang, X. Sun, M. Fan, X. Hu and Z. Dong, *ACS Appl. Mater. Interfaces*, 12, 7285-7294, (2020).
- [13] F. Zhao, K. Murakami, M. Shirai and M. Arai, *J. Catal.*, 194, 479-483, (2000).
- [14] J. P. Stambuli, S. R. Stauffer, K. H. Shaughnessy and J. F. Hartwig, *J. Am. Chem. Soc.*, 123, 2677-2678, (2001).

- [15] P. W. Böhm Volker and A. Herrmann Wolfgang, *Chem. Eur. J.*, 7, 4191-4197, (2001).
- [16] R. A. Sheldon, M. Wallau, I. W. C. E. Arends and U. Schuchardt, *Acc. Chem. Res.*, 31, 485-493, (1998).
- [17] S. Singh and A. Patel, *J. Cleaner Prod.*, 72, 46-56, (2014).
- [18] L. Zhang, Z. Su, F. Jiang, Y. Zhou, W. Xu and M. Hong, *Tetrahedron*, 69, 9237-9244, (2013).
- [19] Z. Shi and X. F. Bai, *Open Mater. Sci.*, 9, 173-177 (2015).
- [20] M. Gholinejad, M. Razeghi and C. Najera, *RSC Adv.*, 5, 49568-49576, (2015).
- [21] B. Abbas Khakiani, K. Pourshamsian and H. Veisi, *Appl. Organomet. Chem.*, 29, 259-265, (2015).
- [22] M. Sarvestani and R. Azadi, *Appl. Organomet. Chem.*, 31, e3667, (2016).
- [23] Z. Hezarkhani and A. Shaabani, *RSC Adv.*, 6, 98956-98967, (2016).
- [24] X.-W. Guo, C.-H. Hao, C.-Y. Wang, S. Sarina, X.-N. Guo and X.-Y. Guo, *Catal. Sci. Technol.*, 6, 7738-7743, (2016).
- [25] V. Kandathil, B. D. Fahlman, B. S. Sasidhar, S. A. Patil and S. A. Patil, *New J. Chem.*, 41, 9531-9545, (2017).
- [26] Y. Monguchi, F. Wakayama, S. Ueda, R. Ito, H. Takada, H. Inoue, A. Nakamura, Y. Sawama and H. Sajiki, *RSC Adv.*, 7, 1833-1840, (2017).
- [27] R. Fareghi-Alamdari, M. G. Haqiqi and N. Zekri, *New J. Chem.*, 40, 1287-1296, (2016).
- [28] R. Tao, S. Miao, Z. Liu, Y. Xie, B. Han, G. An and K. Ding, *Green. Chem.*, 11, 96-101, (2009).
- [29] T. Zhang, B. Li, X. Zhang, J. Qiu, W. Han and K. L. Yeung, *Microporous Mesoporous Mater.*, 197, 324-330, (2014).
- [30] C. Zhang, Y. Leng, P. Jiang, J. Li and S. Du, *ChemistrySelect*, 2, 5469-5474, (2017).
- [31] J. Panpranot, K. Phandinthong, P. Praserttham, M. Hasegawa, S.-i. Fujita and M. Arai, *J. Mol. Catal. A: Chem.*, 253, 20-24, (2006).

CHAPTER 3

Zirconia Supported Stabilized
PdNCLs by LTPA: Synthesis,
Characterization and
Applications to C-C coupling
and Hydrogenation

The outstanding activity of PdTPA/ZrO₂ in both C-C coupling and hydrogenation, encourage us to design another catalyst for the same applications as well as to investigate the effect of addenda atom on the reactions.

In this chapter, we report the synthesis of stabilized PdNCLs by LTPA and its supporting onto surface of zirconia (PdLTPA/ZrO₂) by impregnation and post reduction method. The catalyst was characterized by EDX, TGA, BET, FT-IR, powder XRD, XPS and HRTEM. The efficiency of the catalyst was evaluated as a sustainable heterogeneous catalyst for C-C coupling (SM and Heck) and hydrogenation. Influence of various parameters such as catalyst amount, temperature, pressure, time, base, solvent, solvent ratio was studied for respective reactions to obtain maximum conversion. The catalyst was retrieved by simple centrifugation, regenerated at just 100 °C and reused up to five cycles. The regenerated catalyst was characterized by various characterization techniques to confirm its sustainability. The viability was also examined towards different substrates as well as comparison with the previously reported systems was also surveyed. Further, in order to understand the role of addenda atom, the catalytic activity was compared with PdTPA/ZrO₂.

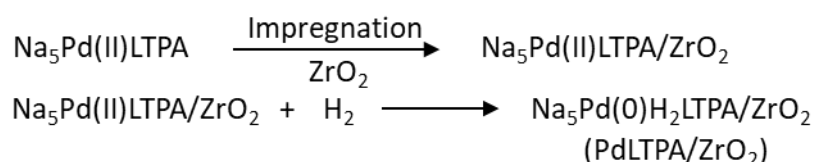
EXPERIMENTAL

Materials

All chemicals used were of A. R. grade. Anhydrous disodium hydrogen phosphate, sodium tungstate dihydrate, acetone, nitric acid, hydrochloric acid, zirconium oxychloride, 25 % (w/v) ammonia, palladium chloride, iodobenzene, phenylboronic acid, styrene, dimethyl formamide, potassium carbonate, cyclohexene, petroleum ether, ethyl acetate and dichloromethane were obtained from Merck and used as received.

Synthesis of PdLTPA supported onto Zirconia

A series of catalysts, containing 10-40 % of Pd(II)LTPA supported on ZrO₂ was synthesized by incipient wet impregnation method. 1 g of ZrO₂ was impregnated with aqueous solution of Pd(II)LTPA (0.1/10-0.4/40 g mL⁻¹ of double distilled water) and dried at 100 °C for 10 h and finally treated under 1 bar H₂ pressure at 40 °C for 30 min using Parr reactor. The obtained materials with 10-40 % loading was designated as 10 % PdLTPA/ZrO₂, 20 % PdLTPA/ZrO₂, 30 % PdLTPA/ZrO₂ (Later, PdLTPA/ZrO₂) and 40 % PdLTPA/ZrO₂, respectively. Reaction scheme for PdLTPA/ZrO₂ synthesis is shown in scheme 2.



Scheme 2 Reaction scheme of PdLTPA/ZrO₂ synthesis.

Catalytic Evaluation

The C-C coupling and hydrogenation reactions were carried out following the same procedure as mentioned in Part-A_Chapter 1.

The effect of loading on all the three reactions was evaluated by varying % loading of PdLTPA (10-40 %) onto ZrO₂. The obtained results (Figure 1) shows that conversion increases with increase in % loading from 10 % to 30 % PdLTPA on ZrO₂. However, a further increase in loading from 30 % to 40 % resulted no change in conversion, which may be due to the blocking of active sites in catalysts. Hence, 30% PdLTPA/ZrO₂ (Later, PdLTPA/ZrO₂) catalyst was selected for detailed characterization and catalytic study.

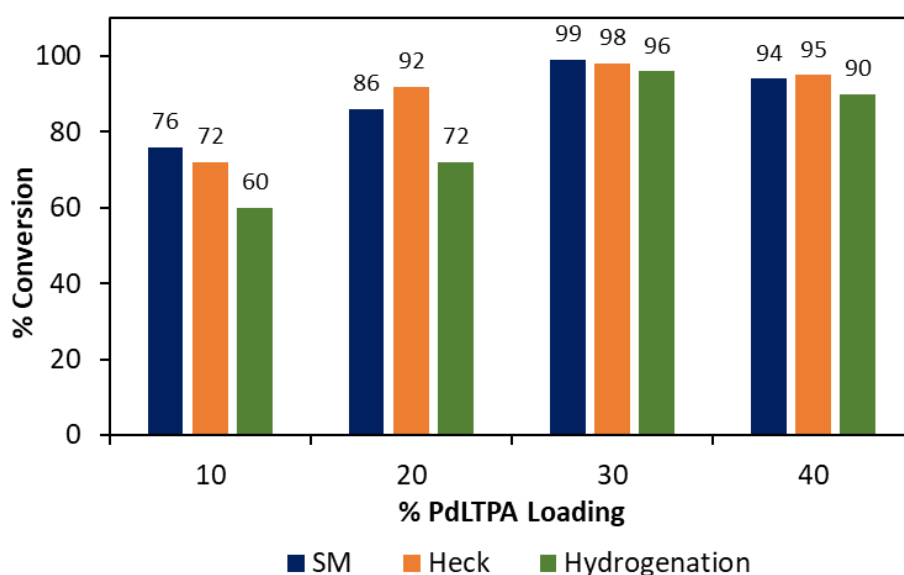


Figure 1 Effect of PdLTPA loading. Reaction condition: *SM coupling*- iodobenzene (1.96 mM), phenylboronic acid (2.94 mM), catalyst (0.0194 mol% Pd), K_2CO_3 (3.92 mmol), $C_2H_5OH:H_2O$ (3:7 mL), temperature (90 °C), time (30 min); *Heck coupling*- iodobenzene (0.98 mM), styrene (1.47 mM), catalyst (0.117 mol% Pd), K_2CO_3 (1.96 mmol), $DMF:H_2O$ (3:2 mL), temperature (100 °C), time (6 h); *Hydrogenation*- cyclohexene (9.87 mmol), catalyst (0.0154 mol% Pd), H_2O (50 mL), temperature (80 °C), H_2 pressure (10 bar), time (5 h).

RESULTS AND DISCUSSION

Catalyst Characterization

The gravimetric analysis of Pd (3.58 wt %) and W (67.34 wt %) for PdLTPA are in good agreement with the theoretical values (3.54 wt % and 67.26 wt %, respectively) as well as EDX values (3.49 wt % and 67.12 wt %, respectively). The EDS value of Na (3.79 wt %) is also resemble with theoretical one (3.82 wt %), which is equivalent to five sodium atoms. For PdLTPA/ ZrO_2 , EDX values for Pd (0.82 wt %), W (15.47 wt %) and Na (0.86 wt %) are also in good agreement with theoretical values, Pd (0.81 wt %), W (15.52 wt %) and Na (0.86 wt %). EDX elemental mapping of the catalysts is shown in figure 2.

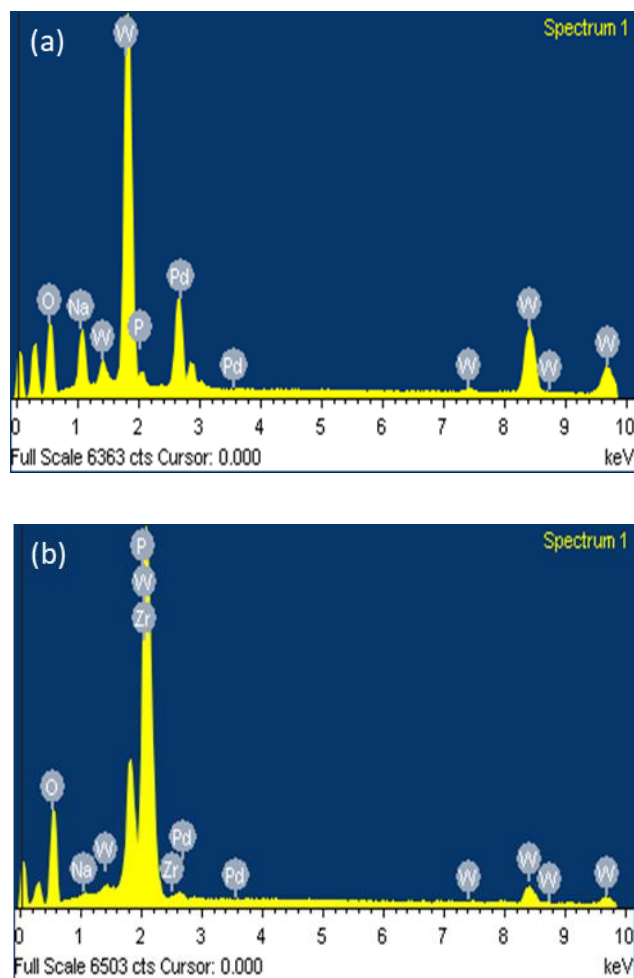


Figure 2 EDX mapping of (a) PdLTPA and (b) PdLTPA/ZrO₂.

TGA of PdLTPA (Figure 3) shows 5.10 % weight loss due to adsorbed water, in the temperature range of 60-110 °C. While, 1.36 % weight loss up to 190 °C, indicating the loss of crystalline water molecules. Whereas, PdLTPA/ZrO₂ shows an initial weight loss of 3.74 % up to 110 °C, indicating the loss of adsorbed water molecules followed by 1.48 % weight loss up to 190 °C because of removal of crystalline water. Besides this, no significant weight loss up to 500 °C, indicates high thermal stability of the catalyst.

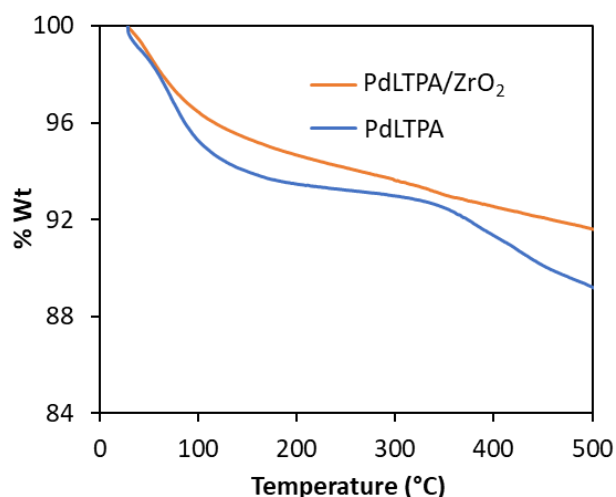


Figure 3 TGA curves.

The FT-IR spectra of ZrO_2 , LTPA, PdLTPA, and PdLTPA/ ZrO_2 are shown in figure 4. Spectrum of ZrO_2 shows broad bands in the region of 1600, 1370, and 600 cm^{-1} attributed to H-O-H and O-H-O bending and Zr-OH bending, respectively. FT-IR spectrum of LTPA exhibits bands at 1088, 1042, 964, 903 and 810 cm^{-1} corresponding to P-O, W=O and W-O-W stretching, respectively. Here, the splitting of P-O bond is due to the lowering of symmetry around central hetero atom phosphorus, indicates the formation of lacunary spices. Whereas, PdLTPA shows bands at 1089, 1043, 957, 903 and 811 cm^{-1} corresponding to P-O, W=O, and W-O-W stretching, respectively. Here, slight shift of the bands may be due to the presence of Pd. FT-IR spectrum of PdLTPA/ ZrO_2 exhibited bands at 1096, 1042, 957, 902, 810 cm^{-1} corresponding to P-O, W=O, and W-O-W stretching vibration frequencies, respectively. Here, the retention of all the characteristic peaks of PdLTPA without any significant shift indicates that basic structure of Keggin unit remains intact even after impregnation as well as post reduction.

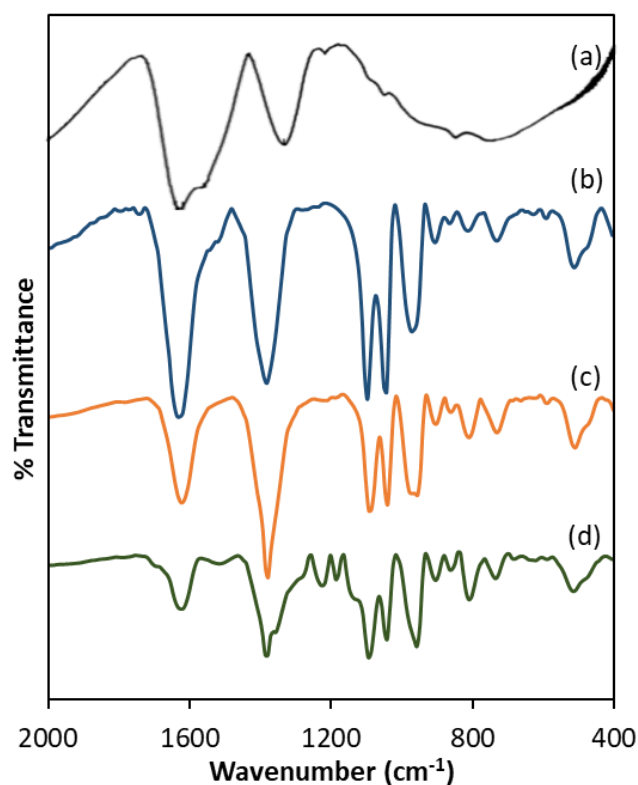


Figure 4 FT-IR spectra of (a) ZrO₂, (b) LTPA, (c) PdLTPA and (d) PdLTPA/ZrO₂.

The value for BET surface area of ZrO₂ was found to be 170 m²/g, whereas, that of PdLTPA/ZrO₂ was 204 m²/g. The observed drastic increase in surface area is due to the presence of PdNCLs onto surface of ZrO₂. The identical N₂ sorption isotherms were also recorded (Figure 5), the identical nature of the isotherms for both, support and designed catalyst, indicate the retention of the basic nature of the catalyst even after impregnation and post reduction treatment. Further, it was reflected in FT-IR.

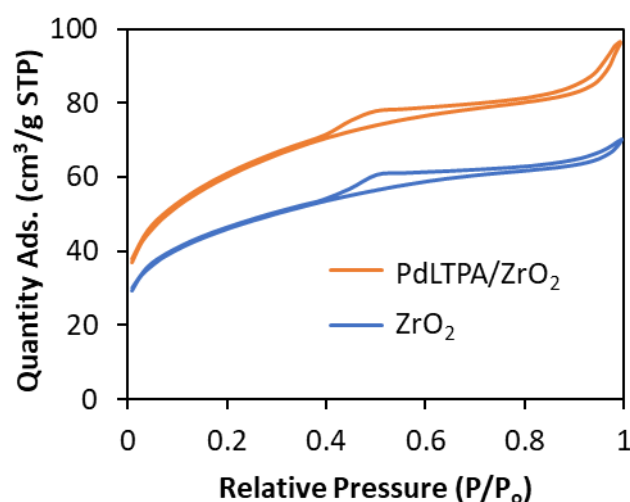


Figure 5 N₂ sorption isotherms.

To study the surface morphology and rate of dispersion in synthesized materials, the XRD patterns of LTPA, PdLTPA, ZrO₂ and PdLTPA/ZrO₂ were recorded (Figure 6). XRD patterns of LTPA shows the characteristic peaks between 2θ range of 20 to 35 degree. Whereas, XRD of PdLTPA shows all the patterns corresponds to LTPA, indicating the retention of Keggin structure. ZrO₂ shows the characteristic broad peak between 20-30, 2θ value. Whereas, in XRD patterns of PdLTPA/ZrO₂, absence of any crystalline peak corresponds to PdLTPA, reveals the homogeneous dispersion of PdLTPA onto surface of ZrO₂. XRD patterns of PdLTPA/ZrO₂ did not reflect any diffraction corresponds to PdLTPA, indicates the high degree of dispersion onto surface of ZrO₂ as well as no sintering of Pd was form during the synthesis.

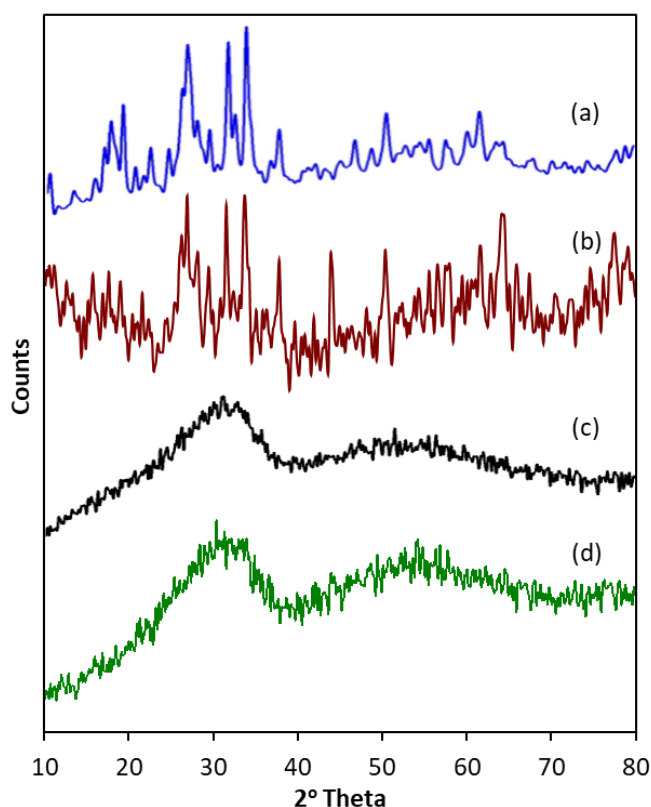


Figure 6 Powder XRD patterns of (a) LTPA, (b) PdLTPA, (c) ZrO₂ and (d) PdLTPA/ZrO₂.

The oxidation state of the Pd, W and O was confirmed by recording high resolution XPS spectra of PdLTPA and PdLTPA/ZrO₂ (Figure 7). Both the catalysts present an intense peak at binding energy 532 eV (Pd3p_{3/2} and O1s) as they contain PdLTPA precursor and ZrO₂ as support, which is in good agreement with the well-known fact that there is direct overlap between Pd3p_{3/2} and O1s peaks [2], and cannot be assigned to confirm the presence of Pd(0). Hence, we have presented full spectra (Figure 7a & 7d) images supporting the presence of Pd(0). To further confirm, the high resolution Pd3d and W4f XPS spectra of both the catalysts were recorded. PdLTPA shows a spin orbit doublet peak of Pd3d at binding energy 335.2 eV (3d_{5/2}) and 340.5 eV (3d_{3/2}), confirming the presence of Pd(0) [3-6]. Whereas, PdLTPA/ZrO₂ shows the doublet peak at 335.2 eV and 340.4 eV, correspond to Pd3d_{5/2} and Pd3d_{3/2}, confirming the presence of Pd(0) onto surface of ZrO₂.

PdLTPA shows (Figure 7c) a well resolved spin-orbit doublet of $W4f_{7/2}$ and $W4f_{5/2}$ at binding energy 35.7 and 37.8 eV (spin-orbit splitting, 2.1 eV), characteristic of W(VI), confirming the presence of W(VI). Similarly, PdLTPA/ ZrO_2 also shows (Figure 7f) a single spin-orbit pair at binding energy 35.6 and 37.7 eV (spin-orbit splitting, 2.1 eV) confirming no reduction of W(VI) during the synthesis [4, 7].

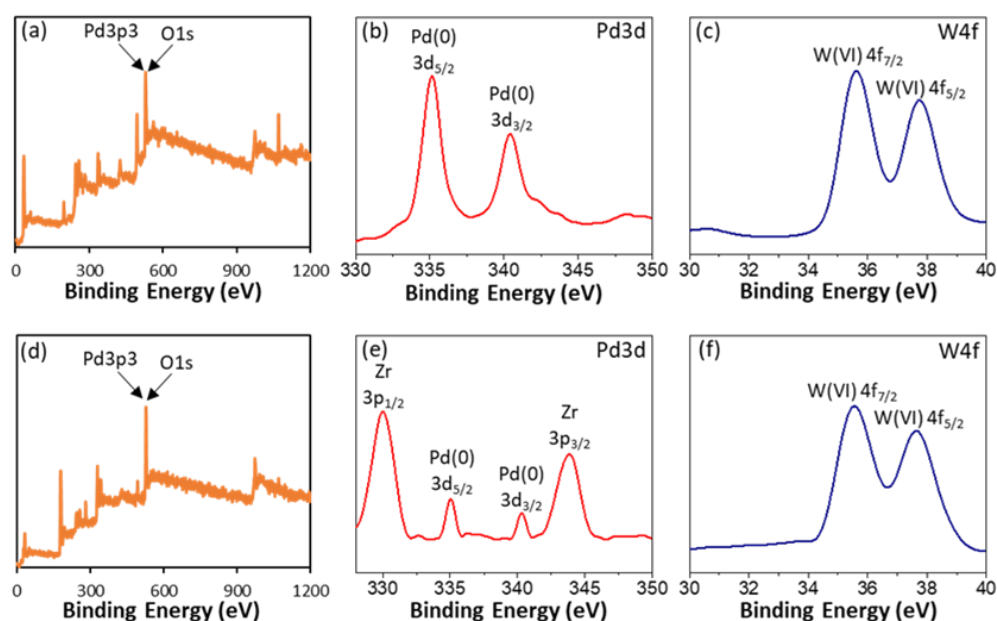


Figure 7 XPS spectra of PdLTPA (a, b and c) and Pd LTPA/ ZrO_2 (d, e and f).

HRTEM images of PdLTPA/ ZrO_2 (Figure 8) are presented at various magnifications. Images clearly indicate the presence of PdNCLs of ~ 2 nm with equidistance homogeneous dispersion onto surface of ZrO_2 without any aggregation.

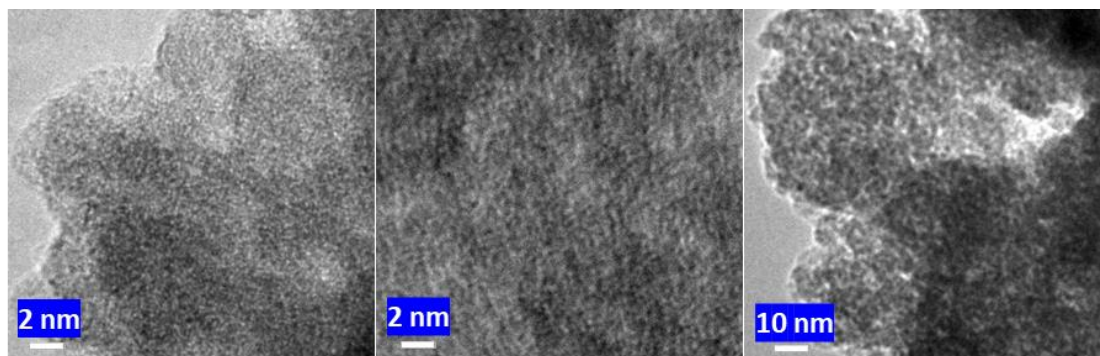


Figure 8 HRTEM images of PdLTPA/ZrO₂.

In summary, FT-IR shows the retention of Keggin structure even after impregnation and post-reduction of the catalyst. The presence of Pd(0) is confirmed by XPS. Further, it confirms the stability of W(VI), during the post reduction of the catalyst. HRTEM confirms the presence of homogeneously dispersed PdNCLs onto surface of ZrO₂.

Catalytic activity

SM Coupling

Iodobenzene (1.96 mmol) and phenylboronic acid (2.94 mmol) were selected as the test substrates and effect of different reaction parameters such as palladium concentration, time, temperature, base, solvent and solvent ratio were studied to optimize the conditions for maximum conversion.

As discussed in previous chapter, we have screened the all parameters thoroughly to achieve maximum % conversion and obtained results are presented in figure 9, table 1 and table 2. The effect of catalyst amount (Pd concentration, figure 9a) was screened between 5-20 mg and results shows that only 5 mg of catalyst (0.0194 mol% Pd) is capable to achieve 99 % conversion. The influence of time on catalytic conversion was screened between 10 min to 40 min as shown in figure 9b, which indicates that 30 min is sufficient for maximum conversion. The effect of temperature (Figure 9c) was studied from

60 to 90 °C and 99 % conversion was obtained at 90 °C. Effect of organic-inorganic bases (Figure 9d) was also studied and K_2CO_3 was found as the best for maximum conversion.

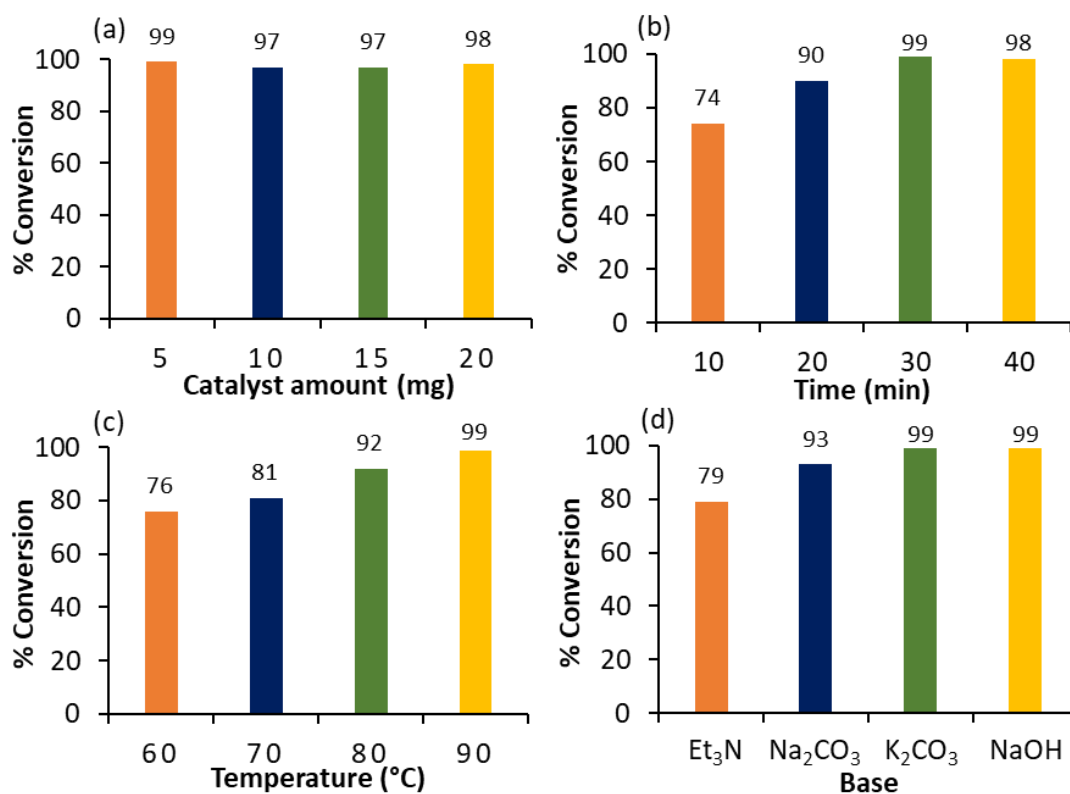


Figure 9 Optimization of parameters for SM coupling. Reaction conditions: (a) Effect of catalyst amount- K_2CO_3 (3.92 mmol), EtOH: H_2O (3:7 mL), time (30 min), temperature (90 °C); (b) Effect of time- catalyst (5 mg), K_2CO_3 (3.92 mmol), EtOH: H_2O (3:7 mL), temperature (90 °C); (c) Effect of temperature- catalyst (5 mg), K_2CO_3 (3.92 mmol), EtOH: H_2O (3:7 mL), time (30 min); (d) Effect of base- catalyst (5 mg), base (3.92 mmol), EtOH: H_2O (3:7 mL), time (30 min), temperature (90 °C).

The effect of different solvent (Table 1) as well as solvent ratio (Table 2) shows that (3:7) mL ratio of EtOH: H_2O is an appropriate solvent for the present system. It should be noted that the explanation will remain the same as discussed earlier chapter.

Table 1 Effect of solvent

Solvent	% Conversion
Toluene	8
Acetonitrile	38
Ethanol	51
H ₂ O	42

Reaction conditions: Catalyst (5 mg), K₂CO₃ (3.92 mmol), solvent (10 mL), time (30 min), temperature (90 °C).

Table 2 Effect of solvent ratio

Ethanol: H ₂ O	% Conversion
1:9	72
2:8	91
3:7	99
4:6	99
5:5	98

Reaction conditions: Catalyst (5 mg), K₂CO₃ (3.92 mmol), time (30 min), temperature (90 °C).

From the above study, the optimized conditions for the maximum % conversion (99) are: iodobenzene (1.96 mmol), phenylboronic acid (2.94 mmol), K₂CO₃ (3.92 mmol), conc. of Pd (3.81×10^{-4} mmol, 0.0194 mol%), substrate/catalyst ratio (5150/1), C₂H₅OH:H₂O (3:7 mL), time (30 min), temperature (90 °C). The calculated TON is 5099 and TOF is 10198 h⁻¹.

Heck coupling

In this case, iodobenzene (0.98 mmol) and styrene (1.47 mmol) were selected as the test substrates. Effect of different reaction parameters such as palladium concentration, time, temperature, base, solvent and solvent ratio was studied to optimize the conditions for maximum conversion. Obtained results are shown in figure 10, table 3 and table 4 and explanation will be the same as discussed in SM coupling section.

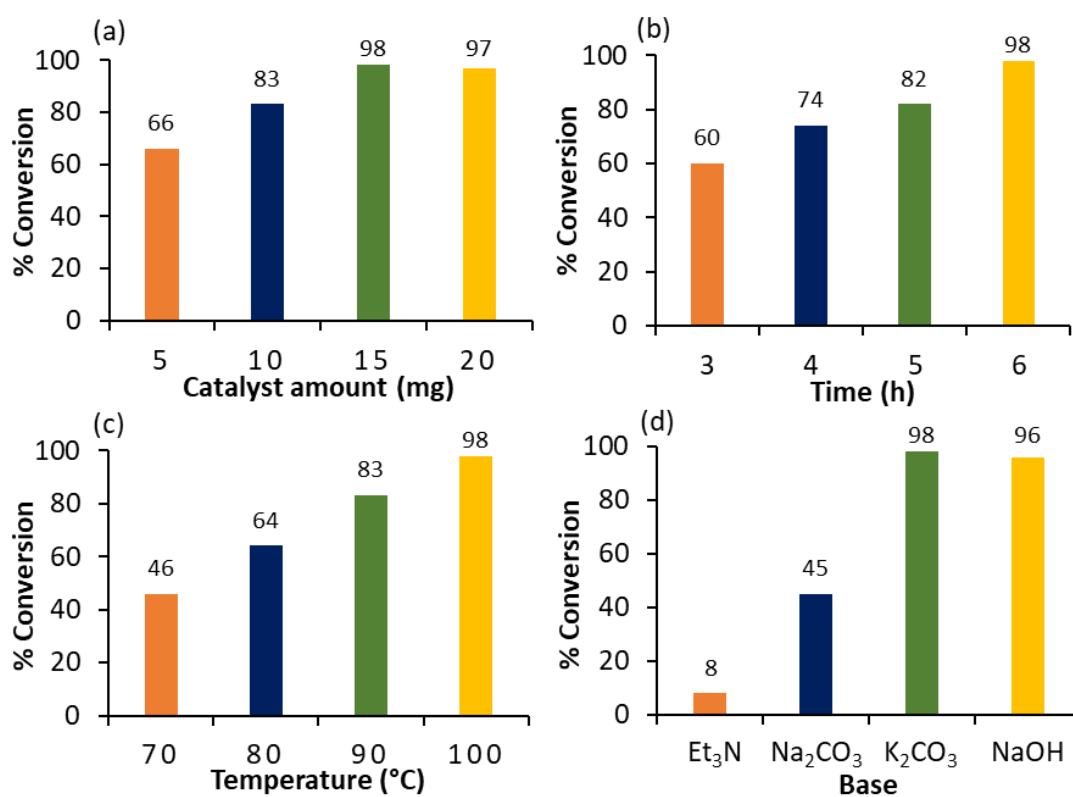


Figure 10 Optimization of Heck coupling. Reaction conditions: (a) Effect of catalyst amount- K₂CO₃ (1.96 mmol), DMF:H₂O (3:2 mL), time (6 h), temperature (100 °C); (b) Effect of time- catalyst (15 mg), K₂CO₃ (1.96 mmol), DMF:H₂O (3:2 mL), temperature (100 °C), (c) Effect of temperature- catalyst (15 mg), K₂CO₃ (1.96 mmol), DMF:H₂O (3:2 mL), time (6 h); (d) Effect of base- catalyst (15 mg), base (1.96 mmol), DMF:H₂O (3:2 mL), time (6 h), temperature (100 °C).

Table 3 Effect of solvent

Solvent	% Conversion
Toluene	4
Ethanol	24
DMF	52
H ₂ O	3

Reaction conditions: Catalyst (15 mg), K₂CO₃ (1.96 mmol), time (6 h), temperature (100 °C).

Table 4 Effect of solvent ratio

DMF: H ₂ O	% Conversion
1:4	34
2:3	72
3:2	98
4:1	83

Reaction conditions: Catalyst (15 mg), K₂CO₃ (1.96 mmol), time (6 h), temperature (100 °C).

The optimized conditions for the maximum % conversion (98) are: iodobenzene (0.98 mmol), styrene (1.47 mmol), K₂CO₃ (1.96 mmol), conc. of Pd (1.14×10^{-3} mmol, 0.117 mol%), substrate/catalyst ratio (858/1), DMF:H₂O (3:2 mL), time (6 h), temperature (100 °C). The calculated TON is 841 and TOF is 140 h⁻¹.

Hydrogenation

To evaluate the efficiency of the catalyst for hydrogenation, cyclohexene (9.87 mmol) was selected as a test substrate. Effect of different reaction parameters such as palladium concentration, time, temperature, pressure and solvent were studied to optimize the conditions for maximum conversion. Obtained results are shown in figure 11 and table 5.

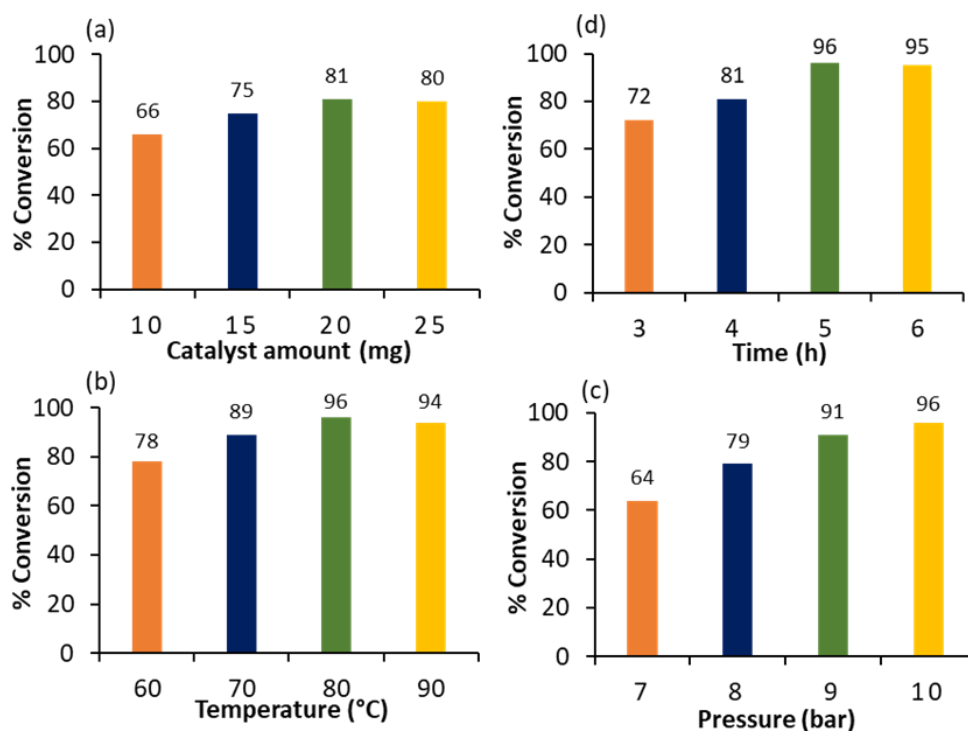


Figure 11 Optimization of cyclohexene hydrogenation. Reaction conditions: (a) Effect of catalyst amount- cyclohexene (9.87 mmol), H₂O (50 mL), time (4 h), temperature (80 °C), H₂ pressure (10 bar); (b) Effect of time- cyclohexene (9.87 mmol), H₂O (50 mL), catalyst (20 mg), temperature (80 °C), H₂ pressure (10 bar); (c) Effect of temperature: cyclohexene (9.87 mmol), H₂O (50 mL), catalyst (20 mg), time (5 h), H₂ pressure (10 bar); (d) Effect of pressure: cyclohexene (9.87 mmol), H₂O (50 mL), catalyst (20 mg), time (5 h), temperature (80 °C).

Table 5 Effect of solvent

Solvent (20: 30) mL	% Conversion
CH ₃ CN: H ₂ O	69
IPA: H ₂ O	95
EtOH: H ₂ O	98
H ₂ O (50 mL)	96

Reaction conditions: cyclohexene (9.87 mmol), catalyst (20 mg), time (5 h), temperature (80 °C), H₂ pressure (10 bar).

The optimized conditions for the maximum % conversion (96) are: cyclohexene (9.87 mmol), H₂O (50 mL), conc. of Pd (1.52×10^{-3} mmol, 0.0154 mol%), substrate/catalyst ratio (6484/1), time (5 h), temperature (80 °C) and H₂ pressure (10 bar). The calculated TON is 6224 and TOF is 1245 h⁻¹.

Control Experiments

In all the three reactions, control experiments were carried out with LTPA, ZrO₂, PdCl₂ and PdLTPA under optimized conditions in order to understand the role of each component and results are shown in table 6. It is seen from the table that LTPA and ZrO₂ were inactive towards the reactions. Almost same conversion was found in the case of PdCl₂, PdLTPA and PdLTPA/ZrO₂ in all reactions. This indicates that Pd is real active species responsible for the reactions and we could succeed in supporting of real active species without any alteration in activity.

Table 6 Control experiment

Catalyst	SM	Heck	Hydrogenation
	% Conversion ^a	% Conversion ^b	% Conversion ^c
LTPA (^a 1.15, ^b 3.46, ^c 4.62 mg)	N. R.	N. R.	N. R.
ZrO ₂ (^a 3.85, ^b 11.54, ^c 15.38 mg)	N. R.	N. R.	N. R.
PdCl ₂	99	97	95
PdLTPA	98	98	94
PdLTPA/ZrO ₂	99	98	96

Reaction conditions. (a) SM coupling: iodobenzene (1.96 mmol), phenylboronic acid (2.94 mmol), catalyst (0.0405 mg Pd, 0.0194 mol% Pd), K₂CO₃ (3.92 mmol), C₂H₅OH: H₂O (3:7 mL), time (30 min), temperature (90 °C); (b) Heck coupling: iodobenzene (0.98 mmol), styrene (1.47 mmol), catalyst (0.1215 mg Pd, 0.117 mol% Pd), K₂CO₃ (1.96 mmol), DMF: H₂O (3:2 mL), time (6 h), temperature (100 °C); (c) Hydrogenation: cyclohexene (9.87 mmol), catalyst (0.162 mg Pd, 0.0154 mol% Pd), H₂O (50 mL), time (5 h), temperature (80 °C), H₂ pressure (10 bar). N. R. – No reaction.

Leaching and Heterogeneity test

The leaching of PdNCLs as well as LTPA from ZrO₂ was checked following the same method as discussed in chapter-2 (Please refer, Page No. 204-205) and found no leaching of either Pd or LTPA from ZrO₂. However, the minor change in % conversion (Table 7) may be due to the instrument error ($\pm 1-1.5$ %). Like in case of PdTPA/ZrO₂ (Chapter-2), in the present case, it was also found that ZrO₂ holds PdLTPA very strongly and does not allow to leach it into the reaction mixture, making it a true heterogeneous catalyst of category C [8].

Table 7 Leaching test

Catalyst	SM	Heck	Hydrogenation
	% Conversion ^a	% Conversion ^b	% Conversion ^c
PdLTPA/ZrO ₂	74 (after 10 min)	60 (after 3 h)	63 (after 2 h)
	73 (after 30 min)	61 (after 6 h)	64 (after 5 h)

Reaction conditions. (a) *SM coupling*: iodobenzene (1.96 mmol), phenylboronic acid (2.94 mmol), catalyst (0.0405 mg Pd, 0.0194 mol% Pd), K₂CO₃ (3.92 mmol), C₂H₅OH: H₂O (3:7 mL), temperature (90 °C); (b) *Heck coupling*: iodobenzene (0.98 mmol), styrene (1.47 mmol), catalyst (0.1215 mg Pd, 0.117 mol% Pd), K₂CO₃ (1.96 mmol), DMF: H₂O (3:2 mL), temperature (100 °C); (c) *Hydrogenation*: cyclohexene (9.87 mmol), catalyst (0.162 mg Pd, 0.0154 mol% Pd), H₂O (50 mL), temperature (80 °C), H₂ pressure (10 bar).

Recyclability and sustainability of the catalyst

Recyclability and sustainability for PdLTPA and PdLTPA/ZrO₂ were studied as described in chapter-2 (Please refer, Page No. 206-207) and the results are described in figure 12. Obtained results show that, while PdLTPA exhibited gradual decrease in % conversion due to leaching of active PdNCLs, PdLTPA/ZrO₂ displayed constant % conversion up to five cycles for all reactions, as in case of PdTPA/ZrO₂ thereby confirming the important role played by the support.

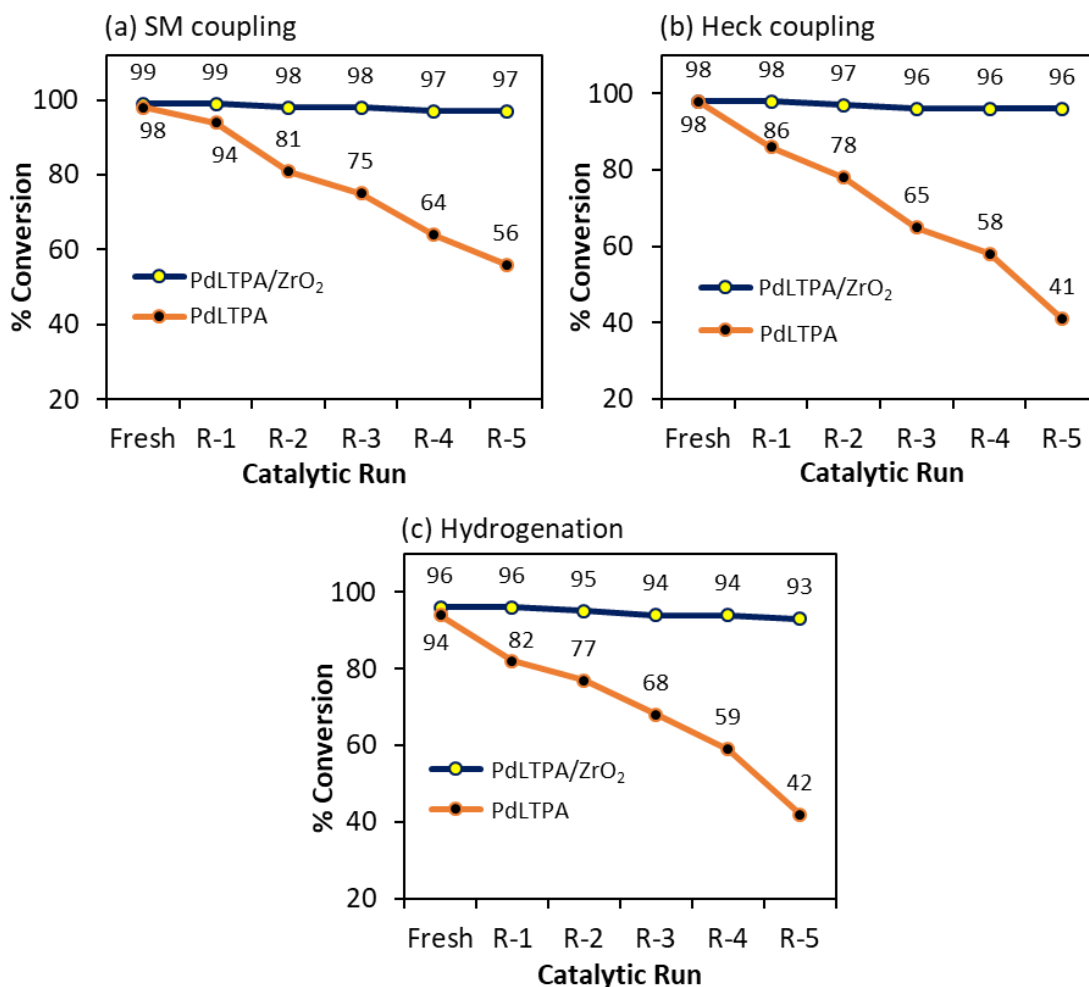


Figure 12 Recycling test. Reaction conditions: (a) *SM coupling*- iodobenzene (1.96 mmol), phenylboronic acid (2.94 mmol), catalyst (0.0405 mg Pd, 0.0194 mol% Pd), K₂CO₃ (3.92 mmol), C₂H₅OH: H₂O (3:7 mL), time (30 min), temperature (90 °C); (b) *Heck coupling*- iodobenzene (0.98 mmol), styrene (1.47 mmol), catalyst (0.1215 mg Pd, 0.117 mol% Pd), K₂CO₃ (1.96 mmol), DMF: H₂O (3:2 mL), time (6 h), temperature (100 °C); (c) *Hydrogenation*- cyclohexene (9.87 mmol), catalyst (0.162 mg Pd, 0.0154 mol% Pd), H₂O (50 mL), time (5 h), temperature (80 °C), H₂ pressure (10 bar).

Characterization of Regenerated catalyst

The stability of the regenerated catalyst was studied by its characterization, such as EDX, FT-IR, BET, XRD and XPS.

For regenerated PdLTPA/ ZrO_2 , the EDX values of Pd (0.81 wt %), W (15.44 % wt) and Na (0.84 wt %) are in good agreement with the fresh one (0.82 wt % Pd, 15.47 wt % W and 0.86 wt % Na), confirming no emission of Pd, W as well as Na from the catalyst during the reaction, confirming no emission of Pd and LTPA from ZrO_2 during the reaction. Elemental mapping is shown in figure 13.

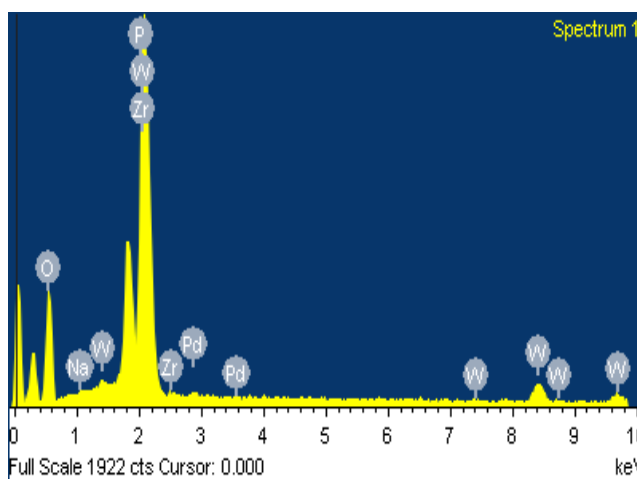


Figure 13 EDX mapping of regenerated PdLTPA/ ZrO_2 .

The FT-IR spectra of the fresh and regenerated catalyst are shown in figure 14. The spectrum of regenerated catalysts shows bands at 1096, 1049, 957, 903, 810 cm^{-1} corresponding to P-O, W=O, and W-O-W stretching vibration frequencies, respectively. Here, the retention of all the characteristic peaks of PdLTPA without any significant shift indicates that basic structure of Keggin unit remains intact even after its repeated use confirming the sustainability of the catalyst. However, the spectrum intensity was found low in case of regenerated catalyst, may be due to the sticking of the substrates, although this might not be significant in the reutilization of the catalyst [9].

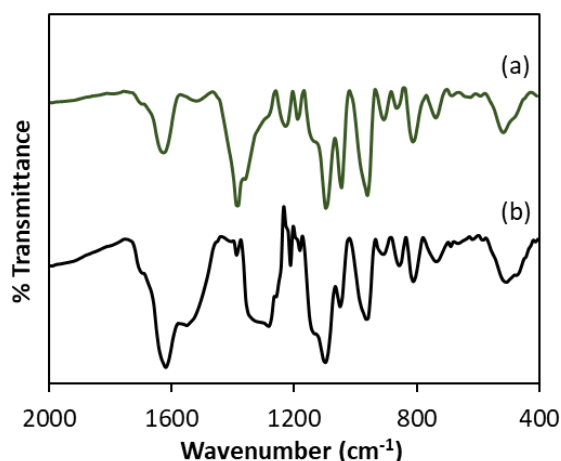


Figure 14 FT-IR spectra of (a) fresh and (b) regenerated PdLTPA/ZrO₂.

Identical BET surface area of fresh (206 m²/g) and regenerated (204 m²/g) catalysts indicates that PdNCLs sites remains intact during the reaction, do not undergo sintering or aggregation. Moreover, no change in N₂ sorption isotherm (Figure 15) of regenerated catalyst in comparison with fresh one proves that there is no alteration in the basic structure of the catalyst.

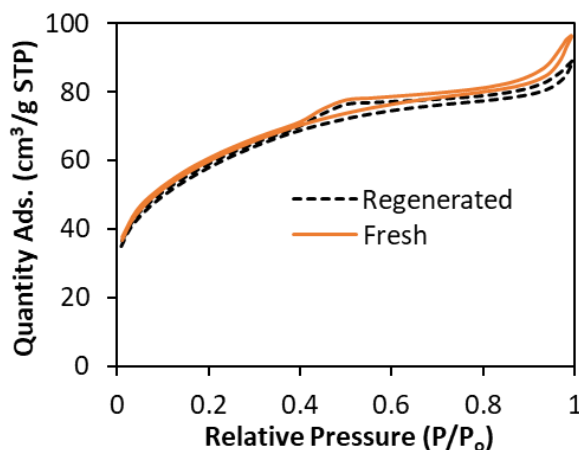


Figure 15 N₂ physisorption isotherms of fresh and regenerated catalysts.

XRD patterns of fresh and regenerated catalyst are shown in figure 16. Obtained results reveal the retention of highly dispersed nature of the catalyst. Absence of any characteristic peaks regarding Pd aggregates as well as LTPA clearly indicates the sustainability of the catalyst during the reaction.

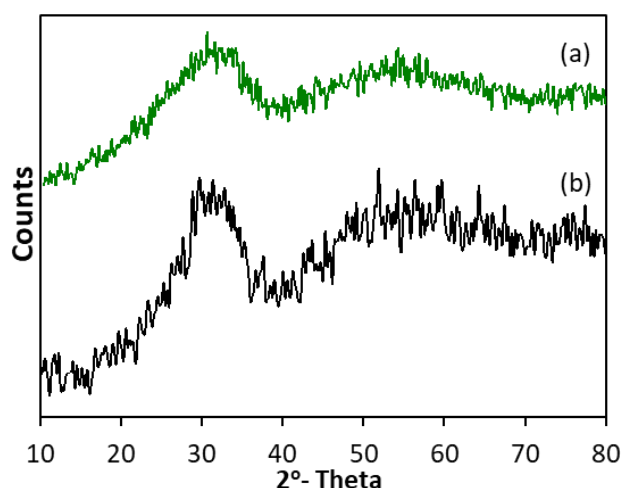


Figure 16 XRD patterns of (a) fresh and (b) regenerated PdLTPA/ZrO₂.

XPS spectra of regenerated PdLTPA/ZrO₂ are displayed in figure 17. The spectra of regenerated catalyst are found to be identical with fresh one (Figure 7), confirms the retention of Pd(0) active species as well as W(VI), which did not undergo reduction during the reaction, indicating the sustainability of the catalyst.

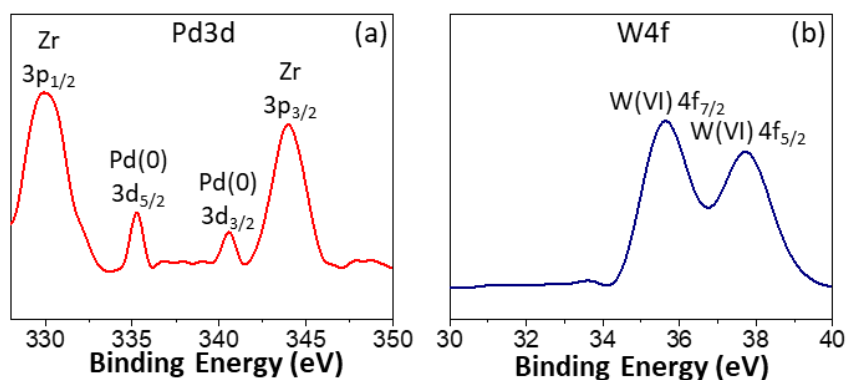


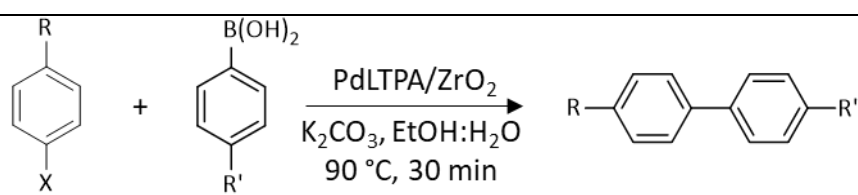
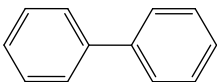
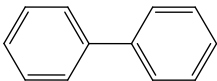
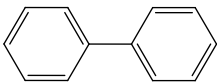
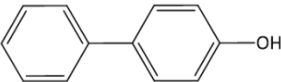
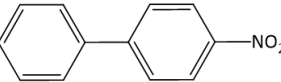
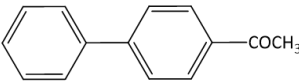
Figure 17 XPS spectra of regenerated PdLTPA/ZrO₂.

In conclusion, FT-IR shows the retention of LTPA structure even after its reuse number of times. XPS and XRD confirm the presence of homogeneously dispersed PdNCLs sites onto surface of ZrO₂. While BET surface area and N₂ sorption curves reveal the unaltered uniform dispersion of PdNCLs with retention of basic structure of Keggin.

Viability of the catalyst

Under the optimized condition, the scope and limitations of substrates were investigated for SM coupling by using different halobenzenes (Table 8) and the similar trend of the activity was found as discussed in the earlier chapter.

Table 8 Substrate study for SM coupling

					
R	X	R'	Product	% Conversion	TON/TOF (h ⁻¹)
H	I	H		99	5099/10198
H	Br	H		63 94 (5 h)	3243/6486 4841/968
H	Cl	H		8 82 (10 h)	412/824 4223/422
OH	Br	H		91	4687/9374
NO ₂	Br	H		99	5099/10198
COCH ₃	Br	H		93	4790/9580

Reaction conditions: Halobenzene (1.96 mmol), phenylboronic acid (2.94 mmol), K₂CO₃ (3.92 mmol), conc. of Pd(0) (0.0194 mol%), substrate/catalyst ratio (5150/1), C₂H₅OH:H₂O (3:7 ml), time (30 min), temperature (90 °C).

Similarly, under optimized conditions, scope and limitations of substrates for Heck coupling were also investigated by using different halobenzenes and styrene derivatives, the obtained results are presented in table 9.

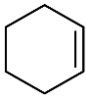
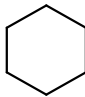
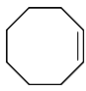
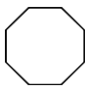
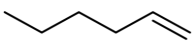
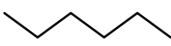
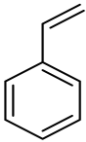
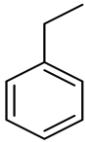
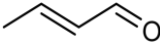

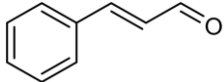
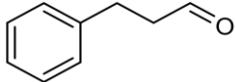
Table 9 Substrate study for Heck coupling

X	R	Product	% Conversion	TON/TOF (h ⁻¹)
I	H		98	841/140
Br	H		71	609/102
			96 (10 h)	824/82
Cl	H		11	94/16
			48 (10 h)	412/41
I	CH ₃		72	618/103
			82 (10 h)	704/70

Reaction conditions: Halobenzene (0.98 mmol), styrene (1.47 mmol), K₂CO₃ (1.96 mmol), conc. of Pd (0.117 mol%), substrate/catalyst ratio (858/1), DMF: H₂O (3:2 mL), time (6 h), temperature (100 °C).

For hydrogenation, the efficiency of the catalyst was evaluated towards different aliphatic and aromatic alkenes. Obtained results (Table 10) shows that, even though all substrates are insoluble in water, present catalyst is highly viable. Ring size effect was observed for the activity of the catalyst. Moreover, the catalyst was found to be active for selective hydrogenation of the C=C bond without tolerating the C=O bond when simultaneously present in the substrates.

Table 10 Substrate study for hydrogenation

Substrate	Product	% Conversion/Selectivity	TON/TOF
		96	6224/1245
		61	3955/791
		76	4928/986
		92	5965/1193
		82/100	5317/1063
		69/100	4474/895

Reaction conditions: Substrate (9.87 mmol), conc. of Pd (0.0154 mol%), substrate/catalyst ratio (6484/1), H₂O (50 mL), time (5 h), temperature (80 °C), H₂ Pressure (10 bar).

Comparison with reported catalyst

Catalytic activity of the present catalyst is also compared with reported catalysts for C-C coupling reactions (Table 11 & 12) in terms of iodobenzene and hydrogenation reaction (Table 13) in terms of cyclohexene as one of the substrates.

It is seen for SM coupling (Table 11), that the present catalyst is superior in terms of mol% of Pd as well as reaction time as compared to all reported catalytic systems.

Table 11 Comparison of catalytic activity for SM coupling with reported catalysts in organic-water solvent mixture with respect to iodobenzene

Catalyst	Pd (mol %)	Solvent	Temp. (°C)/Time (h)	% Conversion/TON /TOF (h ⁻¹)
Pd-ScBTC NMOFs [10]	0.5	C ₂ H ₅ OH: H ₂ O (1:1 mL)	40/0.5	99/194/388
Pd/C [11]	0.37	C ₂ H ₅ OH: H ₂ O (1:1 mL)	40/0.5	99/268/535
Oximepalladacycle catalyst [12]	0.3	C ₂ H ₅ OH: H ₂ O (1:1 mL)	RT/0.3	95/317/1057
Fe ₃ O ₄ /Ethyl-CN/Pd [13]	0.2	C ₂ H ₅ OH: H ₂ O (1:1 mL)	RT/0.2	98/49/245
G-BI-Pd [14]	0.45	C ₂ H ₅ OH: H ₂ O (1:1 mL)	80/0.084	98/219/2613
PdLTPA/ZrO₂ (Present catalyst)	0.0194	C₂H₅OH: H₂O (3:7 mL)	90/0.5	99/5099/10198

In case of Heck coupling (Table 12) also, present catalyst is found superior in terms of the used solvent medium, mol% of Pd, % conversion as well as high TON/TOF.

Table 12 Comparison of catalytic activity for Heck reaction with reported catalysts with respect to iodobenzene

Catalyst	Pd (mol %)	Solvent	Temp. (°C)/Time (h)	% Conversion/TON/TOF (h ⁻¹)
PdTSPc@KP-GO [15]	0.792	H ₂ O (10 mL)	reflux/9	89/111/12
Pd/CNCs [16]	1.412	DMF (10 mL)	40/5	93/65/13
NO ₂ -NHC-Pd@Fe ₃ O ₄ [17]	1.0	CH ₃ CN (5 mL)	80/5	96/96/19
5% Pd/CM [18]	0.2	DMA	80/24	61/3050/127
PFM-Pd [19]	1.7	DMF (3 mL)	120/6	95/56/9
PdLTPA/ZrO₂ (Present catalyst)	0.117	DMF: H₂O (3:2 mL)	100/6	98/841/140

In case of hydrogenation, the true competence of the presented catalyst is also compared with reported systems (Table 13). Liu et al. [20] reported high conversion at a lower temperature, with the utilization of very high H₂ pressure (20 bar) for the reaction compared to present work. Zhang et al. [21] reported the reaction at 35 °C with very poor conversion, moreover a mole % of catalyst was too high. Leng et al. [22] achieved high conversion using formic acid as an *in situ* proton transferring agent with a very high concentration of the Pd compared to the present catalytic system along with very low TON. Panpranot et al. [23] achieved excellent conversion using supercritical CO₂ as a solvent at 60 bar pressure (extremely high condition). Enumerated data of table 13 indicates that the present catalytic system is best one of all reported one in terms of activity under mild reaction conditions.

Table 13 Comparison with the reported catalyst with respect to cyclohexene hydrogenation

Catalyst	Pd (mol%)	Solvent	Temp. (°C)	Pressure (bar)	% Conv./TON/TOF
SH-IL-1.0wt%Pd [20]	0.02	Auto-clave	60	20	99/5000/5000
Pd/MSS@ZIF-8 [21]	0.1738	Ethyl acetate	35	1	5.6/560/93
Pd@CN [22]	2.208	Formic acid	90	(Proton transfer)	96/44/3.67
Pd/SiO ₂ [23]	0.091	CO ₂ (60 bar)	25	10	96/1097/6582
PdLTPA/ZrO₂ (Present catalyst)	0.0154	Water	80	10	96/6224/1245

Comparison study of PdTPA/ZrO₂ and PdLTPA/ZrO₂

In order to compare the activity of the catalysts, both C-C coupling and hydrogenation reactions were carried out under identical experimental conditions. Obtained results (Table 14) are compared in terms of % conversion, TON/TOF.

Table 14 Effect of addenda atom on % conversion, TON/TOF

Catalyst	Total acidic sites (mequi./g)	No. of counter protons	SM coupling		Heck coupling		Hydrogenation	
			% Conv.	TON/TOF	% Conv.	TON/TOF	% Conv.	TON/TOF
PdLTPA/ZrO ₂	4.4	2	99	5099/ 10198	98	841/ 140	79	5186/ 1297
PdTPA/ZrO ₂	4.6	3	97	4996/ 9992	96	824/ 137	94	6171/ 1029

Reaction conditions: *SM coupling*- iodobenzene (1.96 mmol), phenylboronic acid (2.94 mmol), K₂CO₃ (3.92 mmol), conc. of Pd (0.0194 mol%), substrate/catalyst ratio (5150/1), C₂H₅OH: H₂O (3:7 mL), time (30 min), temperature (90 °C); *Heck coupling*- iodobenzene (1.96 mmol), phenylboronic acid (2.94 mmol), K₂CO₃ (3.92 mmol), conc. of Pd (0.117 mol%), substrate/catalyst ratio (858/1), DMF: H₂O (3:2 mL), time (6 h), temperature (100 °C); *Hydrogenation*- cyclohexene (9.87 mmol), conc. of Pd (0.015 mol%), substrate/catalyst ratio (6565/1), H₂O (50 mL), time (4 h), temperature (80 °C), H₂ pressure (10 bar).

In case of C-C coupling, the results (Table 14) show that PdLTPA/ZrO₂ is more active compared to PdTPA/ZrO₂. This can be explained on the basis of total acidic sites. The high activity of PdLTPA/ZrO₂ is attributed to its lower acidity compared to PdTPA/ZrO₂. As base K₂CO₃ was used in the reaction, which is necessary for the transmetallation step for the formation of product, gets neutralized with acidity of the catalyst and lowers the rate of the reaction. As a result, PdLTPA/ZrO₂ is more active than PdTPA/ZrO₂.

In the case of hydrogenation, obtained results (Table 14) show that PdTPA/ZrO₂ is more active than PdLTPA/ZrO₂. This can be explained on the basis of number of counter protons. It is well known that for surface

phenomenon type catalytic hydrogenation, the formation of Pd-H is necessary, higher the formation of Pd-H more the substrates collision for fruitful % conversion. As PdTPA/ZrO₂ consists three hydrogen (in the form of counter protons), which accelerate the formation of Pd-H to enhance the hydrogenation rate, whereas PdLTPA/ZrO₂ has only two counter protons and as a result it activates the reaction moderately.

Activity order of the catalysts is:

C-C Coupling: **PdLTPA/ZrO₂ > PdTPA/ZrO₂**

Hydrogenation: **PdTPA/ZrO₂ >> PdLTPA/ZrO₂**

Conclusion

- Synthesis of stabilized PdNCLs by LTPA (PdLTPA) as well as its supporting onto zirconia (PdLTPA/ZrO₂) was carried out successfully and confirmed by various physico chemical techniques
- The supported catalyst depicts outstanding activity for C-C coupling (SM and Heck) and hydrogenation (> 95 % conversion)
- Leaching and heterogeneity test confirm true heterogeneous nature, regeneration and recycling study shows stable catalytic activity up to five cycles (and can be used for more), whereas EDX, FT-IR, XRD, BET and XPS of regenerated catalyst confirm the sustainability of the catalyst
- Substrate study shows that catalyst is highly viable towards different variety of the substrates
- PdLTPA/ZrO₂ presents superior catalytic activity towards C-C coupling whereas PdTPA/ZrO₂ shows towards hydrogenation compared to each other indicating that acidity of the catalyst plays an important role in the C-C coupling whereas, number of counter protons in hydrogenation reaction

References

- [1] V. Kogan, Z. Aizenshtat, R. Popovitz-Biro and R. Neumann, *Org. Lett.*, 4, 3529-3532, (2002).
- [2] A. V. Matveev, V. V. Kaichev, A. A. Saraev, V. V. Gorodetskii, A. Knop-Gericke, V. I. Bukhtiyarov and B. E. Nieuwenhuys, *Catal. Today*, 244, 29-35, (2015).
- [3] Y. Leng, C. Zhang, B. Liu, M. Liu, P. Jiang and S. Dai, *ChemSusChem*, 11, 3396-3401, (2018).
- [4] R. Villanneau, A. Roucoux, P. Beaunier, D. Brouri and A. Proust, *RSC Adv.*, 4, 26491-26498, (2014).
- [5] L. D'Souza, M. Noeske, R. M. Richards and U. Kortz, *Appl. Catal., A*, 453, 262-271, (2013).
- [6] L. D'Souza, M. Noeske, R. M. Richards and U. Kortz, *J. Colloid Interface Sci.*, 394, 157-165, (2013).
- [7] S. Rana and K. M. Parida, *Catal. Sci. Technol.*, 2, 979-986, (2012).
- [8] R. A. Sheldon, M. Wallau, I. W. C. E. Arends and U. Schuchardt, *Acc. Chem. Res.*, 31, 485-493, (1998).
- [9] S. Singh and A. Patel, *J. Cleaner Prod.*, 72, 46-56, (2014).
- [10] L. Zhang, Z. Su, F. Jiang, Y. Zhou, W. Xu and M. Hong, *Tetrahedron*, 69, 9237-9244, (2013).
- [11] Z. Shi and X. F. Bai, *Open Mater. Sci. J.* 9, 173-177, (2015).
- [12] M. Gholinejad, M. Razeghi and C. Najera, *RSC Adv.*, 5, 49568-49576, (2015).
- [13] B. Abbas Khakiani, K. Pourshamsian and H. Veisi, *Appl. Organomet. Chem.*, 29, 259-265, (2015).
- [14] M. Sarvestani and R. Azadi, *Appl. Organomet. Chem.*, 31, e3667, (2016).
- [15] Z. Hezarkhani and A. Shaabani, *RSC Adv.*, 6, 98956-98967, (2016).
- [16] X. W. Guo, C. H. Hao, C. Y. Wang, S. Sarina, X. N. Guo and X. Y. Guo, *Catal. Sci. Technol.*, 6, 7738-7743, (2016).

- [17] V. Kandathil, B. D. Fahlman, B. S. Sasidhar, S. A. Patil and S. A. Patil, *New J. Chem.*, 41, 9531-9545, (2017).
- [18] Y. Monguchi, F. Wakayama, S. Ueda, R. Ito, H. Takada, H. Inoue, A. Nakamura, Y. Sawama and H. Sajiki, *RSC Adv.*, 7, 1833-1840, (2017).
- [19] R. Fareghi-Alamdari, M. G. Haqiqi and N. Zekri, *New J. Chem.*, 40, 1287-1296, (2016).
- [20] R. Tao, S. Miao, Z. Liu, Y. Xie, B. Han, G. An and K. Ding, *Green. Chem.*, 11, 96-101, (2009).
- [21] T. Zhang, B. Li, X. Zhang, J. Qiu, W. Han and K. L. Yeung, *Microporous Mesoporous Mater.*, 197, 324-330, (2014).
- [22] C. Zhang, Y. Leng, P. Jiang, J. Li and S. Du, *ChemistrySelect*, 2, 5469-5474, (2017).
- [23] J. Panpranot, K. Phandinthong, P. Praserttham, M. Hasegawa, S. I. Fujita and M. Arai, *J. Mol. Catal. A: Chem.*, 253, 20-24, (2006).

OVERALL COMPARISON

Comparison of activity

In order to check the activity order, coupling and hydrogenation reactions were carried out over all synthesized catalysts Pd-TPA/ZrO₂, Pd-LTPA/ZrO₂, PdTPA/ZrO₂ and PdLTPA/ZrO₂ using similar active amount of Pd under identical experimental conditions and obtained results are compared in terms of % conversion, TON/TOF (Table 1).

Table 1 % Conversion, TON/TOF for C-C coupling

Catalyst	% Conversion	TON/TOF (h ⁻¹)	No. of counter protons	Total acidic sites (Bulk acidity) (mequiv./g)
Pd-TPA/ZrO ₂	^a 99	^a 10325/20650	3	4.2
	^b 99	^b 860/143		
PdTPA/ZrO ₂	^a 86	^a 8865/17730	3	4.7
	^b 96	^b 834/139		
PdLTPA/ZrO ₂	^a 92	^a 9595/19190	2	4.4
	^b 97	^b 843/140		
Pd-LTPA/ZrO ₂	^a 62	^a 6466/12932	7	5.1
	^b 70	^b 608/101		

^a**SM coupling:** Reaction conditions- iodobenzene (1.96 mmol), phenylboronic acid (2.94 mmol), K₂CO₃ (3.92 mmol), conc. of Pd (0.0096 mol%), substrate/catalyst ratio (10429/1), C₂H₅OH: H₂O (3:7) mL, temperature (80 °C), time (30 min).

^b**Heck coupling:** Reaction conditions- iodobenzene (0.98 mmol), styrene (1.47 mmol), K₂CO₃ (1.96 mmol), (3.92 mmol), conc. of Pd (0.115 mol%), substrate/catalyst ratio (869/1), DMF: H₂O (3:2) mL, temperature (100 °C), time (6 h).

Table 1 shows that among all, Pd-TPA/ZrO₂ is highly active for both the reactions and this can be explained on the basis of total acidic sites (Bulk acidity).

The high activity of Pd-TPA/ZrO₂ is attributed to its lower acidity compared to all synthesized catalysts. As the acidity increases, present base i.e. K₂CO₃ in the reaction, necessary for the transmetallation step to give the products, gets neutralized and lowers the rate of the reaction. It is very interesting to note down that even though the number of counter protons for Pd-TPA/ZrO₂ and PdTPA/ZrO₂ is same (three), their value of bulk acidity is different and hence consisting of different catalytic activity. This observed difference in bulk acidity is attributed to different amount of W present. EDX results show that Pd-TPA/ZrO₂ consists 16.87 wt % of W (Please refer, Page No. 68) whereas, PdTPA/ZrO₂ consists 17.36 wt % (Please refer, Page No. 186). The observed difference in tungsten is due to use synthetic method. In PdTPA/ZrO₂, salt was synthesized and then impregnated onto zirconia while, in Pd-TPA/ZrO₂, it consists of two steps: (i) impregnation of TPA onto ZrO₂ (TPA/ZrO₂) and (ii) exchange with the available protons of TPA/ZrO₂. Higher the W amount would mean higher the bulk acidity and as a result PdTPA/ZrO₂ has more total acidic sites and represents lower activity as compared to that of Pd-TPA/ZrO₂.

The activity order of all catalysts towards C-C cross coupling is:

Activity order	Pd-TPA/ZrO₂ >> PdLTPA/ZrO₂ >> PdTPA/ZrO₂ >> Pd-LTPA/ZrO₂			
No. of Counter protons	3	2	3	7
Total acidic sites	4.2	4.4	4.7	5.1

It also shows that the nanocatalyst synthesized by exchange method is better.

Hydrogenation

Obtained results (Table 2) show that Pd-LTPA/ZrO₂ is highly active amongst all synthesized catalysts. This can be explained on the basis of number of counter protons.

Table 2 % Conversion, TON/TOF for hydrogenation

Catalyst	% Conversion	TON/TOF (h ⁻¹)	Number of Protons
Pd-TPA/ZrO ₂	15	4,377/2189	3
Pd-LTPA/ZrO₂	96	28,010/14005	7
PdTPA/ZrO ₂	14	4085/2042	3
PdLTPA/ZrO ₂	8	2334/1167	2

Reaction conditions: cyclohexene (9.87 mmol), conc. of Pd (0.0034 mol%), substrate/catalyst ratio (29177/1), H₂O (50 mL), temperature (50 °C), H₂ pressure (10 bar), time (2 h).

The surpassing activity of Pd-LTPA/ZrO₂ is attributed to highest number of counter protons. It is well known that for surface phenomenon type catalytic hydrogenation, % conversion depends on the formation of Pd-H, higher the formation of Pd-H more fruitful collision of substrates, which enhance % conversion. As Pd-LTPA/ZrO₂ consists seven hydrogen (in the form of counter protons), which accelerate the formation of Pd-H to enhance the hydrogenation rate, whereas PdLTPA/ZrO₂ has only two counter protons and as a result it activates the reaction moderately.

Activity order of the catalysts:

Activity order Pd-LTPA/ZrO₂ >> Pd-TPA/ZrO₂ ≡ PdTPA/ZrO₂ >> PdLTPA/ZrO₂
No. of Counter protons 7 3 3 2

Here also, the nanocatalyst synthesized by ion exchange method is found to be superior as compared to that by salt method.

